INVESTIGATION OF DUAL-MODE SPACECRAFT PROPULSION BY MEANS OF IONIC LIQUIDS

by

BRIAN RUSSELL DONIUS

A THESIS

Presented to the Faculty of the Graduate School of the

MISSOURI UNIVERSITY OF SCIENCE AND TECHNOLOGY

In Partial Fulfillment of the Requirements for the Degree

MASTER OF SCIENCE IN AEROSPACE ENGINEERING

2010

Approved by

Joshua L. Rovey, Advisor
David W. Riggins
Umit O. Koylu

ABSTRACT

Analytical and numerical investigations of the performance of a series of potential dual-mode propulsion systems using ionic liquids are presented. Chemical bipropellant performance of select propellants is determined using NASAs Chemical Equilibrium with Applications. Comparison of the predicted specific impulse of ionic liquids with hydrazine and unsymmetrical dimethylhydrazine shows that the ionic liquid propellants have 3-12% lower specific impulse when paired with nitrogen tetroxide. However, when paired with hydroxylammonium nitrate, the specific impulse of the ionic liquids is 1-4% lower than that of hydrazine and unsymmetrical dimethylhydrazine paired with nitrogen tetroxide. Analytical investigation of an electrospray electric propulsion system shows that if ionic liquids are capable of operating in an almost purely ionic regime, they can provide very high specific impulse (~6000 sec). The predicted chemical and electric performance data are used in conjunction with system mass estimates to predict the system level performance of three dual-mode systems. Results indicate that the dual-mode systems are capable of producing higher change in velocity than traditional systems for any combination of chemical or electrical propulsion at the cost of time. Specifically, if 80% of the velocity change is accomplished by using electrical propulsion, a hydroxylammonium nitrate monopropellant electrospray system produces 190% more change in velocity than a traditional system consisting of a hydrazine monopropellant and xenon Hall effect thruster. This 190% increase in maximum velocity change comes at the cost of 750% more time thrusting for the hydroxylammonium nitrate system.

ACKNOWLEDGMENTS

I would like to recognize the support and tireless efforts I received from Dr. Joshua Rovey while pursuing my course of study. I would also like to acknowledge, Dr. David Riggins and Dr. Umit Koylu, for both accepting the position of committee members and for more than any other professors shaping the course of my undergraduate career. For its financial support, the Missouri Space Grant is especially acknowledged. For their encouragement and giving me the opportunity for hands on research that I would otherwise not have experienced, I would like to thank the members of RZSS AFRL Edwards AFB.

Over the course of twenty three years of life, numerous faculty, staff, colleges, and friends have contributed to what I have become as an engineer and more importantly as a person. Although there is simply insufficient space to thank them all properly, I hope that through my conduct, I showed them the respect which they disserved. To all the members of my vast family, for their never ending support and encouragement of me in the pursuit of my dreams, in the full knowledge that my success would take me from them, a mere thanks is woefully insufficient but it is offered here in small payment of that great debt.

TABLE OF CONTENTS

LIST OF ILLUSTRATIONS

Page

LIST OF TABLES

Page

NOMENCLATURE

Symbol	Description
F_{tu}	Allowable material strength
d	Capillary diameter
ΔV	Change in velocity
L	Characteristic cone length
r*	Charge relaxation length
P_c	Combustion chamber pressure
K	Conductivity
k_1	Constant for Ganan-Calvo current equation
k_d	Constant for Ganan-Calvo droplet equation
ρ	Density
ρ_p	Density of chemical propellant
ρ_m	Density of tank structural material
ε	Dielectric constant
D_d	Droplet diameter
E_n	Electric field normal to the cone surface
E_s	Electric field tangential to the cone surface
c_{chem}	Exhaust velocity of chemical propulsion system
c_{elec}	Exhaust velocity of electric propulsion system
FEEP	Field emission electric propulsion
Q	Flow rate
m_0	Full spacecraft initial mass
$f(\varepsilon)$	Function relation governing current emission
$G(\varepsilon)$	Function relation governing droplet size
e	Fundamental charge
g_0	Gravitational constant
α_ρ	Inertial coefficient
$\dot{M}_i$	Mass flow rate of ion i
M_{ct}	Mass of chemical propellant tank

M_p	Mass of propellant
m_{f1}	Mass of spacecraft after chemical burn
m_{f2}	Mass of spacecraft after electric thrusting
M_{et}	Mass of xenon electric propellant tank
T_m	Melting temperature
MW	Molecular weight
ξ	Non-dimensional current
λ	Non-dimensional current
η	Non-dimensional flow rate
R_ρ	Non-dimensional inertial domain term
r_j	Non-dimensional jet radius
Π_μ	Non-dimensional viscosity coefficient
R_σ	Non-dimensional surface tension domain term
R_μ	Non-dimensional viscosity domain term
ε	Nozzle expansion ratio
R_A	Percent of the total mass flow rate that is pure ions
ε_0	Permittivity of free space
P_t	Propellant tank pressure
PIR	Purely Ionic Regime
R_{jet}	Radius of cone jet
Z	Radius of cone jet Ganan-Calvo derivation
R_c	Radius of curvature for Taylor cone
R	Radius of droplet
P2/P1	Ratio of nozzle exit pressure to combustion chamber pressure
K	Ratio of specific heat
δ	Slenderness parameter
ISP	Specific Impulse
σ	Surface Tension
α	Taylor cone half angle
T	Thrust
T_{chem}	Thrust of chemical propulsion

T_{elec}	Thrust of electric propulsion
t	Time required to effect change in velocity
R’	Universal gas constant
V_A	Velocity of the pure ion
V_B	Velocity of the first solvated state
α_μ	Viscosity coefficient
$\Delta\varphi$	Voltage
V_{xe}	Volume of xenon propellant

1. INTRODUCTION

This thesis summarizes research conducted in the area of dual-mode spacecraft propulsion. A combination of high-thrust chemical and high-specific impulse electric propulsion into a single dual-mode system has the potential to greatly enhance spacecraft mission capability by allowing the spacecraft to adapt to changing mission propulsion requirements. Ideally, the combined system would share both hardware and propellant to provide the greatest reduction in system mass and maximize flexibility in the spacecraft thrust history. By possessing a common fuel a dual-mode chemical, electric propulsion system could trade high-thrust for high-specific impulse as the mission needs developed. Thus, research was restricted to identifying a propellant that could act as a fuel for both chemical and electric spacecraft propulsion, to estimate its performance in both modes and quantify any advantages that result over traditional systems.

In this thesis, the methods, processes, and results of the research are described. In section 1 a summary and a brief history of the class of fuels that became the focus of the research is provided. The methods by which chemical propulsion performance estimated are related and results are discussed in section 2. An introduction to the concept of electrospray propulsion and a review of current methods of predicting performance are presented in section 3. Candidate dual-mode systems are identified and mass budgets are constructed for each system in section 4. The systems are then compared to identify the advantages of each. Overall conclusions and potential avenues for future work are identified in section 5.

1.1. IONIC LIQUIDS

An ionic liquid is either an organic or inorganic salt in a molten (liquid) state. Because of its molten state, the cation and anion of the salt dissociate, but the overall liquid remains quasi-neutral. All salts obtain this state if heated to the proper temperature, but there is a subgroup known as room-temperature ionic liquids that can remain liquid at or below 293 K. Although ionic liquids have been known since 1914, recent developments in chemistry have increased the number of known ionic liquids into the hundreds [1]. The exact mechanism for this molten salt behavior has yet to be

identified, making the prediction of ionic liquid properties difficult. In general, however, ionic liquids have high conductivity, high viscosity, and negligible vapor pressure.

Current research is investigating ionic liquids as replacements for traditional explosives and rocket propellants and volatile industrial solvents in chemical processing [2, 3]. Although most professionals consider ionic liquids benign, a large group of researchers recently highlighted the combustibility of many ionic liquids as they approach decomposition temperature [4]. This work also pointed out that the rate of combustion of several ionic liquids increases dramatically when the ionic liquids are sprayed rather than combusted as a pooled sample. Other articles have suggested that ionic liquid hydroxylammonium nitrate (HAN) may be used as a monopropellant substitute for hydrazine [5-7]. These analyses show that the performance of HAN in both pure and mixed forms is similar to that of hydrazine. Lastly, hypergolic behavior has been reported for several ionic liquids when combined with traditional space storable oxidizers [8-10].

Ionic liquids have also been investigated as electrospray propellants [11-13]. Ionic liquids for electrospray application were initially investigated because of their low vapor pressure. Previous electrospray liquids had relatively high vapor pressure and would boil off the emitter. Interest in this application of ionic liquids has prompted multiple studies exploring plume emission of electrospray ionic liquids. Results have shown that an ionic liquid spray can approach a purely ionic regime (PIR) of emission similar to that found in field emission electric propulsion [13].

1.2. DUAL MODE PROPULSION

The main goal of a dual-mode propulsion system is to reduce spacecraft mass and enhance flexibility through the use of common system resources. Examples of common resources include hardware and propellant. The modes of propulsion can be characterized by the tasks to be performed by the propulsion system during a mission. These tasks include, but are not limited to, high-thrust orbit transfer maneuvers, low-thrust station keeping, low-thrust orbital transitions, and precision low-thrust pulses for attitude control. Although the dual-mode concept for spacecraft has been qualitatively discussed for some time, focus research on the topic has been all but nonexistent.

One of the few instances in which dual-mode propulsion has been applied is the Mars Global Surveyor [14]. However, this system consisted of two chemical systems, a bi and monopropellant thruster. The system was developed on a tight budget and a rushed schedule dictated by the loss of the Mars Observer craft. The system consisted of a common fuel bipropellant thruster and catalyst monopropellant thruster, a detailed schematic can be seen Figure 1-1. The bipropellant thruster was used in conjunction with aero-braking to bring the probe into orbit around Mars, and the monopropellant system was used for attitude control. The propellant common to both thrusters was hydrazine which permitted for the integration of three identical and readily available tanks, thus reducing costs [14]. Dual-mode propulsion was selected for this mission based not on improved performance, but on a desire to speed up development, cut costs, and ease integration issues presented by the smaller size of the Delta II launch vehicle selected for the mission. Although the Mars Global Surveyor does represent a dual-mode system, its use of traditional hypergolic propellants and catalyst monopropellant thrusters leaves little room for improved performance; therefore, new concepts for dual-mode propulsion are investigated.

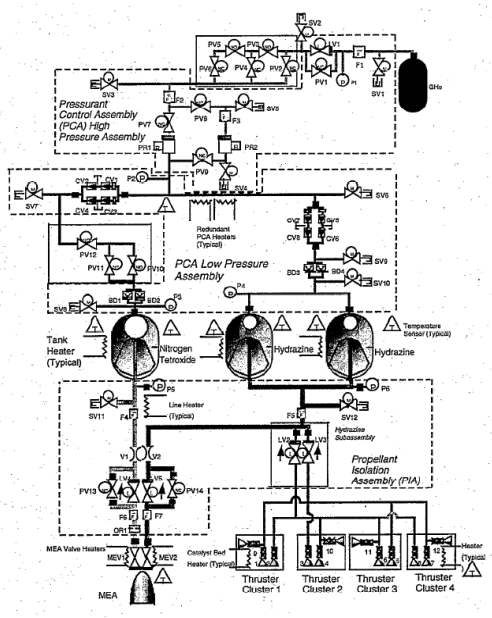

Figure 1-1: Mars Global Surveyor Propulsion Schematic

2. CHEMICAL PROPULSION ANALYSIS

2.1. METHODOLOGY

This work uses the NASA Glenn Research Center's Gordon-McBride Chemical Equilibrium with Applications (CEA) code to analyze the chemical combustion and rocket performance of multiple bipropellant combinations [15]. Specifically, ionic liquid fuels and oxidizers are paired with conventional fuels and oxidizers; CEA is then used to determine the chamber temperature and product chemical properties. Using ideal equations the performance measures of specific impulse, density impulse, and thermal storability are determined and compared to assess the capability of ionic liquids to act as substitutes for traditional chemical propellant combinations. Lastly, a comparison of the predictions of CEA to historical test stand data is conducted to help quantify what performance could be expected from an actual ionic liquid based chemical bipropellant system.

2.2. INVESTIGATED FUELS

Ten different ionic liquids are selected for analysis based on data available in literature. To evaluate the capabilities of an ionic liquid fuel in a chemical propulsion system, the fundamental properties, such as heat of formation, melting point, and density must be determined. Because investigation of the combustion properties of ionic liquids has only recently begun to receive attention, knowledge of heat of formation of these liquids is limited. Thus, 1-butyl-3-methylimidazolium dicyanamide and 1-butyl-3-methylpyrrolidinium dicyanamide are selected as two of the ionic liquids fuels. Additionally, 1-butyl-3-methylimidazolium dicyanamide has been reported to have hypergolic reactions with standard storable oxidizers [10].

The heat of formation of both dicyanamide ionic liquids was determined through calorimeter tests and calculations using the quantum chemistry program Gaussian 3[16-17]. Reported results show a difference of approximately 1% between the calculated and experimental data. Heats of formation for eight energetic ionic liquids based on 5-aminotetrazolate have also been determined [19]. To permit a comparison with current space storable propellants, hydrazine and unsymmetrical dimethylhydrazine (UDMH) are

also evaluated. Hydrazine has the best performance of all traditional storable fuels, but it is highly toxic and notoriously unstable. The performance of UDMH is only slightly inferior to that of hydrazine, but UDMH has a larger storable temperature range and greater stability. Table 2-1 summarizes all thermodynamic data for these propellants.

Table 2-1. Thermochemical data for fuel and oxidizers investigated

Fuel	Fuel Name	Formula	H_{fg}, $kJmol^{-1}$	Density, gcm^{-3}	Melting Point, K
	Hydrazine	N_2H_4	-	1.01	275
	UDMH	$C_2H_8N_2$	-	0.79	216
1	1-Butyl-3-methylimidazolium Dicyanamide	$C_{10}H_{15}N_5$	363.40	1.06	267
2	1-Butyl-3-methylpyrrolidinium Dicyanamide	$C_{11}H_{20}N_4$	218.90	1.02	223
3	Hydrazinium 5-aminotetrazolate	CH_7N_7	383.60	1.48	398
4	Guanidinium 5-aminotetrazolate	$C_2H_8N_8$	205.40	1.54	399
5	Aminoguanidinium 5-aminotetrazolate	$C_2H_9N_9$	302.30	1.51	366
6	Guanylguanidinium 5-aminotetrazolate	$C_3H_{10}N_{10}$	306.90	1.41	414
7	4-Amino-1H-1,2,4-triazolium 5-aminotetrazolate	$C_3H_7N_9$	565.00	1.62	387
8	4-Amino-1-methyl-1,2,4-triazolium 5-aminotetrazolate	$C_4H_9N_9$	546.00	1.46	249
9	4-Amino-1-ethyl-1,2,4-triazolium 5-aminotetrazolate	$C_5H_{11}N_9$	523.40	1.39	235
10	1,5-Diamino-4-methyl-1,2,3,4-tetrazolium 5-aminotetrazolate	$C_3H_9N_{11}$	655.10	1.57	444
	Oxidizers				
	Nitrogen Tertroxide (NTO)	N_2O_4	-	1.44	261.95
	White Fuming Nitric Acid (WFNA)	HNO_3	-	1.33	231.6
	Inhibited Red Fuming Nitric Acid (IRFNA)	83%HNO_3 +14% N_2O_4+ 2.4% H_2O + .6% HF	-	1.59	216
	Hydroxylammonium nitrate (HAN)	NH_3OHNO_3	-79.68	1.83	316.05

2.3. INVESTIGATED OXIDIZERS

Four oxidizers are selected for the combustion analysis. One of the oxidizers, HAN, is an ionic liquid. The other three are common in current state of the art chemical rocket systems; these are nitrogen tertroxide (NTO), white fuming nitric acid (WFNA), and inhibited red fuming nitric acid (IRFNA). NTO is a highly toxic, storable space oxidizer with extensive flight heritage, and in most reactions it provides the best performance. WFNA is essentially pure nitric acid doped with a small percentage of hydrofluoric acid to permit storage in a variety of container materials. In general, WFNA does not perform as well as NTO; however, although it is corrosive, it is relatively benign. In terms of percentage by mass, IRFNA is 83% HNO3, 14% N2O4, 2.4% H2O, and 0.6% HF. In general, IRFNA‘s performance is the same as that of WFNA, but its melting point is much lower. The ionic liquid HAN is selected because of the aforementioned interest in HAN-based monopropellant systems. For combustion analysis, HAN is considered as an oxidizer in a pure liquid state at 316.05 K. The thermodynamic data for the oxidizers is summarized in Table 2-1.

2.4. PERFORMANCE CRITERIA AND SIMULATIONS

The measures of performance selected for investigation here are specific impulse (ISP), density impulse, and storability. ISP is defined as the thrust per unit weight flow rate of propellant; it indicates how efficiently a system uses propellant. For ideal flows, it is determined from (eq. 2.1) [19]. Although the performance of the propellants for rocket propulsion is being assessed assuming that the system is in space the existence of a finite nozzle area ratio ε requires that the finite pressure ratio between the nozzle exit and the chamber be determined. This pressure ratio shown in equation 2.1 is determined by solving the transcendental equation (eq. 2.2) by assuming an area ratio (ε). Because of the assumption of constant ratio of specific heats and molecular weight the ISP reported is the frozen flow case. Density impulse takes into account how easily the oxidizer-fuel combination can be stored by multiplying the ISP by the average storage density of fuel and oxidizer combination. This gives a measure of performance per unit volume of storage. For this project the storability of the propellant is described qualitatively as the need for additional heating or cooling of the propellant to maintain liquid phase in the

storage tanks. Storability is important for reducing strain on the power system of the satellite and preventing excessive propellant loss due to boil-off. For this study, storability is defined quantitatively as the ratio of the melting point temperature of hydrazine to the melting point temperature of the fluid (eq. 2.3). A value greater than one indicates that a propellant is at least as storable as hydrazine, whereas a value less than one indicates that additional heating of the propellant is required. These measures of performance can be determined only if the chemical composition and thermodynamic state of the exhaust stream from the rocket combustion chamber are known.

$$ISP = \frac{\sqrt{\left(2k/k-1\right)\left(RT_0/MW\right)\left(1-P_2/P_1^{(k-1)/k}\right)}}{g_0} \tag{2.1}$$

$$1/\varepsilon = \left(\frac{k+1}{2}\right)^{\frac{1}{k-1}} \left(\frac{P_2}{P_1}\right)^{\frac{1}{k}} \sqrt{\frac{k+1}{k-1}\left(1-\frac{P_2}{P_1}\right)^{\frac{k-1}{k}}} \tag{2.2}$$

$$Storability = \left(\frac{T_{m,N_2H_4}}{T_{m,Fluid}}\right) \tag{2.3}$$

The NASA Chemical Equilibrium with Applications (CEA) code is used to determine the performance of each propellant combination. This program has been under continual development since the late 1950s and enables the user to determine equilibrium composition and adiabatic flame temperature for any reaction [15]. A recent addition to the program also allows the user to define a new fuel given the heat of formation and molecular composition. Since the gaseous heat of formation is required the energy needed to convert the propellants from a liquid to a gas phase is neglected. A series of 1536 simulations are performed using CEA by varying chamber pressure, equivalence ratio, and propellant combination for a fixed expansion ratio (ε) of 40.

2.5. CHEMICAL PERFORMANCE ESTIMATES

The chamber pressure is varied between 150 psia and 600 psia because these are typical levels in on-orbit engines [20]. Figure 2-1 shows performance varied little with chamber pressure. This is to be expected because such relatively small pressures cannot greatly affect the product species dissociation. Therefore, all subsequent analyses are restricted to the 300 psia case.

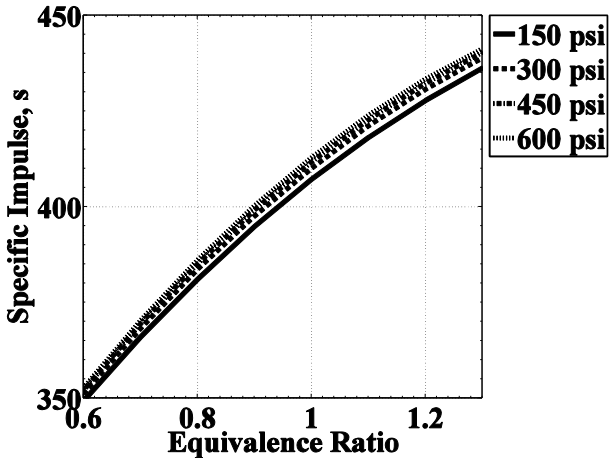

Figure 2-1: Effect of chamber pressure on ISP H2/LOX

For the 48 propellant combinations, the mixture ratio is varied between 0.6 and 1.3 to determine the peak performance for each combination. An equivalence ratio of unity (stoichiometric) represents the point of complete combustion. Generally, peak performance is far to the right of the stoichiometric condition. This result is common for rocket performance because as excess fuel is introduced to the system, molecular weight decreases faster than chamber temperature. Table 2-2 and Table 2-3 summarize the results for all oxidizer fuel combinations. The performance values are scaled with respect to the peak performance of hydrazine when combined with NTO (333, s and 406, g-

s/cm^3). For example, the ISP of UDMH-NTO is 97% of that obtained for hydrazine-NTO.

Table 2-2. Summary of chemical propulsion – NTO and HAN oxidizer

	NTO		HAN		
	Specific Impulse,	Density Impulse,	Specific Impulse,	Density Impulse,	Storability,
Fuel	-	-	-	-	-
Hydrazine	1.00	1.00	1.03	1.14	1.00
UDMH	0.97	0.85	1.01	0.97	1.27
1	0.88	0.91	0.99	1.13	1.03
2	0.94	0.95	0.99	1.11	1.23
3	0.96	1.16	1.00	1.36	0.69
4	0.90	1.10	0.96	1.35	0.69
5	0.92	1.11	0.97	1.34	0.75
6	0.91	1.07	0.97	1.29	0.66
7	0.93	1.16	0.98	1.40	0.71
8	0.93	1.12	0.98	1.33	1.10
9	0.93	1.09	0.98	1.31	1.17
10	0.94	1.16	0.98	1.38	0.62

Results show that hydrazine and UDMH provide higher ISP than any of the ionic liquids investigated here, regardless of the oxidizer. In simulations, however, hydrazine and UDHM combusted with HAN oxidizer provides higher ISP than when combusted with NTO. With NTO oxidizer, the ionic liquid fuels have 3-12% lower ISP than that of hydrazine and UDMH. Results show that NTO performs better than IRFNA and WFNA as an oxidizer for any given fuel with the single exception of 1-butyl-3-methylimidazolium dicyanamide, which has only a small gain of five seconds ISP. IRFNA and WFNA perform almost identically for all propellant combinations. When combined with HAN for ideal combustion, all fuels perform better; however, no ionic

liquid HAN combination performs better than the baseline hydrazine-NTO case. However, the prediction that HAN performs better than NTO warrants further investigation.

Table 2-3. Summary of chemical propulsion – IRFNA and WFNA oxidizer

	IRFNA		WFNA	
Fuel	Specific Impulse, -	Density Impulse, -	Specific Impulse, -	Density Impulse, -
Hydrazine	0.96	1.00	0.96	0.92
UDMH	0.93	0.85	0.93	0.79
1	0.90	0.96	0.90	0.88
2	0.90	0.95	0.90	0.87
3	0.93	1.18	0.93	1.07
4	0.88	1.13	0.88	1.00
5	0.89	1.14	0.89	1.02
6	0.88	1.09	0.88	0.98
7	0.90	1.20	0.90	1.08
8	0.90	1.14	0.90	1.03
9	0.90	1.11	0.90	1.01
10	0.91	1.19	0.91	1.07

In terms of density impulse, the ionic liquids perform better than traditional propellants, especially when combined with IRFNA and HAN. This improved performance is due to the greater density of the ionic liquids in comparison to that of hydrazine or UDMH. Density impulse indicates how easily an oxidizer-fuel combination can be stored. High density makes these propellant combinations ideal for small-volume budgeted systems with proportionally high mass budgets.

Analysis indicates that storability of ionic liquids is a major difficulty. Propellants 1, 2, 8, and 9 show storability equal to or greater than that of hydrazine. The remaining six propellants are not storable space propellants; therefore, they are dropped from

consideration in the remainder of the study. With a storability factor of 0.87, HAN is not necessarily a storable propellant. However, because it is substantially closer to hydrazine than any other ionic liquid that failed the criteria (next closest is 0.75), HAN is the subject of further analysis.

2.6. UNCERTAINTY ANALYSIS

Although CEA has been highly regarded for its predictive capabilities, its performance predictions must still be assessed for accuracy. To quantify the difference in the code performance predictions and real systems, a series of test cases are used to compare the predictions with actual engine performance for systems found in the Chemical Propulsion Information Agency (CPIA) engine manual [20]. Given the mixture ratio, expansion ratio, and chamber pressure, the predicted ISP for equilibrium flow is compared to the actual performance (Figure 2-2).

Error present in the analysis is difficult to quantify but its sources are readily understood. First, the theory used in the design of CEA will have some limitations and numerical error will exist no matter the methods used. Thus, there is an inherent error present in CEA itself. Values of heat of formation for each of the ionic liquids examined have some experimental or theoretical error associated with them depending on the methods used. The test stand data retrieved from the CPIA will have experimental error associated in the measurement of thrust and mass flow rate, thus error will be present in the ISP reported.

Quantification of the error present in CEA would represent an extensive research project unto itself and is not conducted here. The error present in the CPIA engine test data would be all but impossible to determine. The data represents the culmination of dozens of tests conducted by hundreds of individuals over the course of decades, with varying levels of documentation. Thus, no concrete numbers for experimental error can be defined for the CPIA data. The effect of error present in the heat of formation used to determine chemical performance can be quantified. For example, the value for heat of formation of fuel 2 has a reported experimental error of ±3.4 kJ/kmol. By considering this variation in heat of formation, the resultant error in frozen flow ISP for fuel 2 is ±0.06 s. Since error present in the inputs is negligible and the errors associated with the test stand

data and CEA are not readily or possible to quantify only a comparison of the CEA to test stand data is possible. Thus, this does not represent an actual quantification of error but only a method for more conservative estimate of performance.

Figure 2-2 shows that as thrust level increases, the accuracy of the simulation increases; this occurs because a larger thrust chamber dictates that a smaller percentage of the fluid is exposed to the non isentropic effects of high heat transfer rate and boundary layers that develop along the walls of chamber and nozzle. For engines with thrust levels below 100 lbf (typical of small spacecraft), the ISP values predicted by CEA are 15.6% higher on average than those indicated by test data, with a standard deviation of 3.7%. A 19.3% reduction in ISP from the data shown in Table 2-2 is used for the remainder of the study to allow for a more conservative estimate of ISP and represents a factor of safety of one standard deviation.

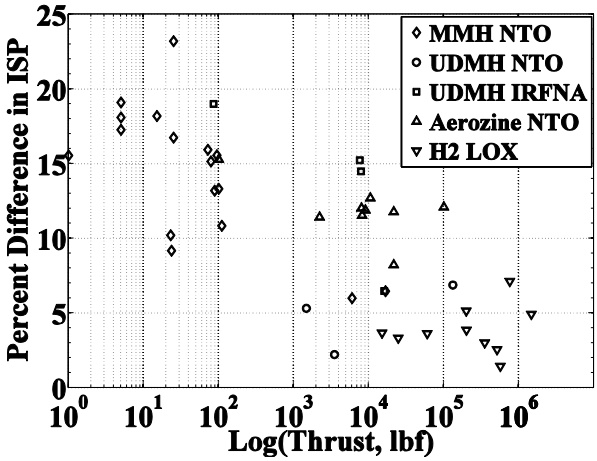

Figure 2-2: Percent difference between CEA and Test Engine Data

3. ELECTRIC PROPULSION ANALYSIS

3.1. INTRODUCTORY CONCEPTS IN ELECTROSPRAY PROPULSION

A dual-mode propulsion system with common propellant must have an electric propulsion system that can operate with a combustible fuel. This investigation focuses on ionic liquids as possible electric propulsion propellants by means of electrospray. After examination of the electrospray process a series of existing electrospray models are summarized to show their limited use for ionic liquid electrospray. These models being inadequate, results of tests on ionic liquids similar to the ionic liquids proposed in this investigation are used to predict the electric propulsion performance of an electrospray thruster.

3.1.1. Electrospray Thrusters. Electrospray is the generation of fine droplet emission by means of an applied electrostatic field. This process has seen application in a variety of fields, including but not limited to mass spectrometry, micro manufacturing and pharmaceuticals. Historically, the modern electrospray thruster has its roots in field emission electric propulsion (FEEP) developed in the 1960's as an alternative to the far better known ion thruster or Hall effect thruster [21]. This system produced propulsion by placing liquidized metal such as cesium in the presence of an intense electric field. When the field was applied a stream of pure ions was formed that would then be accelerated through a potential on the order of 100 kV. The result was a high specific impulse but low thrust on the order of a micro-newton. A drawback to this small thrust was the limit on total thrust of the system. Each emitter was on the order of millimeters and with the high voltage, arcing became a serious issue. Due to the need for higher thrust electric propulsion and the fore mentioned packing difficulties, FEEP research was essentially discontinued in favor of the ion thruster.

Research in the area of electrospray technology for space propulsion was put on hold until the early 1990's. Experiments conducted in other areas of application led Dr. Fernandez de la Mora of Yale University to conclude that electrospray of polar solute doped with metallic salts could produce a capable propulsion system [22]. Rather than relying on field ionization these systems work on the principal of creating a liquid with free ions present. An example of this would be to dissolve lithium chloride in ethylene

glycol, thus a solution of free ions is created. The advantage of these systems was that, instead of requiring on the order of hundreds of kilovolts like FEEP engines, emission of ionized material could be accomplished on the order of 2 kV. Another advantage was the state micro manufacturing which had developed rapidly in the intervening years since the research on FEEP. Now reliable production of emitter sizes of micrometers could be obtained rather than millimeters of the 1960s. This higher emitter density and lower operating voltages made possible higher total thrust systems. However unlike the FEEP, this thruster relied not on pure ion emission but on the ejection of finite drops from a micro fluidic phenomenon known as a Taylor cone.

3.1.2. Taylor Cones and Solution Based Electrospray. This Taylor cone is a micro fluid structure that was first noted by Zeleny in the 1910's [23]. What Zeleny noticed was that fluids in the presence of a strong electric field will evolve in to a conical structure that will emit a micro jet. Much later in the 1960's G.I. Taylor investigated these formations using both mathematical and experimental methods and determined that for conducting fluids a cone angle of 49.29 degrees would always occur [23]. However, later research showed that highly conducting fluids did not obey this constant and therefore the terminology of "cone jet" was introduced. It was later shown by Fernandez de la Mora that highly conducting fluids would produce a space charge effect on the structure effectively reducing this Taylor angle [23].

A cone jet (still often called a Taylor cone despite the discrepancy in angle of the cone) is generally produced by first filling a capillary tube (emitter, syringe) such that a hemispherical protrusion exists at the tip of the tube. From here a potential difference is set up between the emitter and extractor plate. Once formed, the Taylor cone does exhibit a hysteresis effect, whereby the voltage can be reduced below the start up voltage. As voltage is increased beyond start up the conical shape proceeds to deform and protrude further out from the emitter. This stressed jet condition often results in the formation of many Taylor cones from the single meniscus.

Generally put the characteristics of the jet are determined by the flow rate through the cone only and the voltage only determines if cone jet can exist. This independence between voltage and flow rate is crucial to the performance of the electrospray thruster. At the initial start up condition, a fine jet will be emitted from the cone. As this jet travels

downstream, it will begin to destabilize and form a series of fine droplets with diameters of the order of the jet. Depending on the flow rate the distribution of droplet size can vary greatly. As flow rate is increased the jet diameter increases and results in larger droplet sizes while also resulting in effectively in only one size of droplet. A decrease in the flow rate will result in an overall thinning of the jet and reduction in size of the droplets emitted. If flow rate is varied to greatly from the value necessary to create a stable Taylor cone the cone will tend to destabilize resulting in the return to the hemispherical structure or the expulsion of large quantities of fluid.

When the micro jet destabilizes it has been found that secondary processes occur upon the drops themselves. Evidence tends to point to the Rayleigh limit as the maximum charge a droplet can hold [24]. Once the droplet is emitted the rate of solvent evaporation accelerates and the diameter of the drop will rapidly decrease. Once a critical diameter is reached a "Columbic" explosion occurs in which the majority of charge on the drop is lost in axial emission. This resultant droplet system of parent and daughters will continue to undergo this process until collision ends the flight of the drop. This breakdown behavior is counterproductive for the production of high exhaust velocities.

The performance of the doped polar solutions as electrospray propellants has been reported previously and has shown rather varied potential in specific impulse (ISP). Depending on the emission droplet size it can vary from as low as several hundred seconds ISP to the low thousands. The extent to which ISP increases is primarily governed by the development of low mass high charge daughters, as describe previously. Additional problems develop from the finite vapor pressure of the polar solvents. At reduced pressures of space the propellant can be lost through evaporation out of Taylor cones. Despite the low performance this style thruster is already slated to be used on the LISA mission because of its ability to produce repeatable low level thrust for precision station keeping.

3.1.3. Ionic Liquid Based Electrospray. Electrospray of ionic liquids was initially investigated to correct the issue of low vapor pressure of most of the solutions used in various applications [25]. What was found through testing was that a spray of an ionic liquid could actually yield a nearly pure ionic regime (PIR) of emission similar to that found in FEEP. Through time of flight analysis and mass spectrometry it was found

that at certain conditions only ions of the form $Cation^{+}$ $(Cation\text{-}Anion)_N$ were being emitted. Here N is the degree of solvation of ions ranging typically from 0 to 3. Were a value of N = 0 represents the pure ion, with larger values representing the number of neutral pairs carried along by the ion. This result opens up the possibility of greatly increasing the performance for the electrospray thruster by permitting higher ISP.

When high flow rates are used, ionic liquids behave in a similar manner to that of solution based electrospray. As flow rate is decreased, TOF analysis points to a greater decrease in the production of droplets and an increase in the production of pure ions. Pure ionic emission is apparent only when the jet emission has ceased entirely and the cone has reformed into an equal-potential surface. However, PIR is not universal amongst ionic liquids. At room temperature only, EMI-BF4 and EMI-IM have been reported to approach this regime [13, 25]. A wider group of ionic liquids has been found to produce PIR emission at elevated temperatures but PIR has not been reported for liquids possessing relatively high viscosities [22].

3.2. PRESENT ANALYSIS METHODOLOGIES FOR ELECTROSPRAY

With the goal of predicting the capabilities of an ionic liquid based dual mode propulsion system, it is necessary to predict the performance of electrospray. Presented in section are detailed descriptions of the methodologies currently used to predict the performance of doped solvent electrospray thrusters. It is shown that none of the existing methods currently are capable of predicting performance of ionic liquids, especially near PIR.

3.2.1. Experimentally Derived Scaling Laws. The most common methodology of predicting electrospray performance is based on experimentally formulated scaling laws. To date, two experimentally derived scaling laws have been proposed by, Fernandez de la Mora and Loscertales (1994) and Ganan-Calvo (1994) [23, 27]. Fernandez de la Mora and Loscertales started from dimensional analysis, while Ganan-Calvo started from one dimensional flow equations.

The properties used to determine these equations were density, viscosity, conductivity, surface tension, dielectric constant, and flow rate. To examine the behavior of the electrospray three non-dimensional parameters for flow rate, spray current and

viscosity were derived by Fernandez de la Mora and Loscertales (eq. 3.1-3.3). Ganan-Calvo decided on non-dimensional parameters for current, jet radius and a factor for the slenderness (eq. 3.4-3.6). After examining their respective data, both groups came to the conclusion that viscosity would not be a factor except in the case where its value is exceptionally high $\Pi_\mu > 0.3$.

$$\eta = \sqrt{\frac{\rho Q K}{\gamma \varepsilon \varepsilon_0}} \tag{3.1}$$

$$\xi = \frac{I}{\gamma \sqrt{\frac{\varepsilon_0}{\rho}}} \tag{3.2}$$

$$\Pi_\mu = \frac{\sqrt[3]{\left(\frac{\gamma^2 \rho \varepsilon \varepsilon_0}{K}\right)}}{\mu} \tag{3.3}$$

$$rj = \sqrt[3]{\frac{Q\sqrt{\varepsilon}\varepsilon_0}{\pi^2 K}} \tag{3.4}$$

$$\delta = \frac{\varepsilon_0 \gamma}{\rho Q K} \tag{3.5}$$

$$\lambda = \frac{I \sqrt[4]{\varepsilon}}{\sqrt{8KQ\gamma}} \tag{3.6}$$

Prediction of spray current for both groups resulted in a proportionality of $(QK\gamma/\varepsilon)^{1/2}$. In the case of Fernandez de la Mora, this proportionality took the form of (eq. 3.7). The functional form of $f(\varepsilon)$ can be seen in Figure 3-1, apparently showing a plateau in emitted current for high dielectric constant (highly polarized) fluids. Ganan-Calvo results produced the proportionality in (eq. 3.8). Which, rather than approaching a

constant grew for all polarities investigated Figure 3-1. A third group, Chen and Pui (1997) derived their own f(ε) from test data (eq. 3.9) [28].

$$I = f(\varepsilon)\sqrt{\frac{QK\gamma}{\varepsilon}} \tag{3.7}$$

$$I = k_1 \sqrt[4]{\varepsilon}\sqrt{\frac{QK\gamma}{\varepsilon}} \tag{3.8}$$

$$I = -449 - 0.021\varepsilon + 157\sqrt[6]{\varepsilon} + \frac{336}{\sqrt[6]{\varepsilon}} \tag{3.9}$$

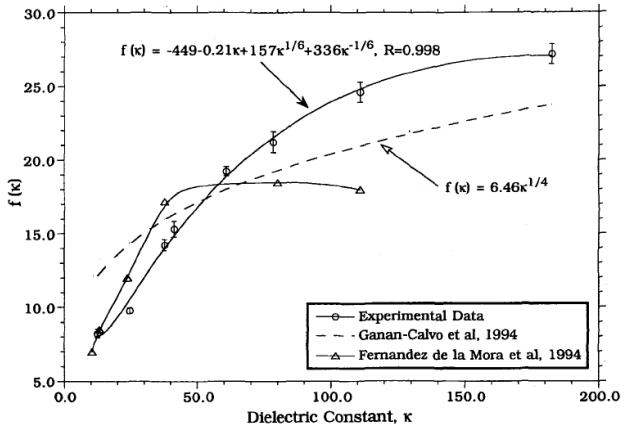

Figure 3-1: Comparison of f(ε) [28]

Both Fernandez de la Mora and Chen used a similar set of solvents for their experiments, yet their results varied greatly. Chen proposed the possibility that the ion mobility for the different additives used to control conductivity might have resulted in the variation. In the case of Fernandez de la Mora lithium chloride was used and in the case of Chen, the additive used was nitric acid. This supposes that the current has two

contributors, convection and conduction. In this case the conduction current would be dictated by the mobility of the ions in additives used and convection would be dictated by the current carried along in the bulk flow. Chen continues on to use a simple order of magnitude analysis to support this claim.

In the case of droplet size, both Fernandez de la Mora and Ganan-Calvo proposed scaling with the charge relaxation length r* (eq. 3.10), where Q is the flow rate. In the case of Fernandez de la Mora the scaling was accomplished by a function G(ε), which represents the change in the diameter of the jet over the change in r*. Fernandez de la Mora did not actually derive this G(ε) but Chen empirically generated it based on high speed images of droplet emission and found the form (eq. 3.11). Ganan also found a value for the constant k_1 to be 1.66 in a similar manner.

$$D_d = G(\varepsilon) r^* = G(\varepsilon) \sqrt[3]{\frac{Q \varepsilon \varepsilon_0}{K}} \tag{3.10}$$

$$D_d = \frac{k_d \sqrt[3]{\frac{Q \varepsilon \varepsilon_0}{K}}}{\sqrt[6]{\varepsilon}} \tag{3.11}$$

3.2.2. Mathematically Derived Scaling Laws. In addition to the fore mentioned scaling laws a purely mathematical formulation was provided by Ganan-Calvo [29]. First by examining the necking and slender jet region of the Taylor cone Gaan-Calvo was able to derive an equation (eq. 3.12) for the momentum of the jet. In this equation z is the axial position downstream, Z is the radius of the jet, En and Es are the electric fields normal and along the surface of the cone and, β is the ratio of the fluid dielectric constant to that of vacuum. Each term shown in the equation (eq. 3.12) represents the effects surface tension, inertia, viscosity, tangential electrostatic surface stress and axial component of normal electrostatic surface stress respectively.

$$\frac{\mathrm{d}}{\mathrm{dz}}\left(\frac{\sigma}{Z} + \frac{\rho Q^2}{2\pi^2 z^4}\right) + \frac{6\mu Q}{\pi Z^2}\frac{d}{dz}\left(\frac{1}{Z}\frac{dZ}{dz}\right) = \frac{z\varepsilon E_n E_s}{Z} + \frac{\varepsilon}{2}\frac{d}{dz}\left(E_n{}^2 + (\beta - 1)E_s{}^2\right) \tag{3.12}$$

After considering that jet break should take place far away from the origin ($d\xi/dz=>0$) equation 3.12 can be reduced and transformed into equation 3.13. Equation 3.13 represent the total current being emitted by the jet and is formally an Eigen value problem. The author then divides the cone jet into two regions necking and the developed jet. Examining the resulting jet far downstream he defines three potential dominate physical non-dimensional quantities (eq. 3.14a-c) surface tension, inertial and viscous. It is then shown by examination of cone necking region that for solutions to be consistent across both regions they must also be either dominate due to electrostatic suction or polarization forces.

$$I = \frac{2Q\varepsilon 0}{z} E_n + \pi Z^2 K E_s \tag{3.13}$$

$$R_\rho = \frac{\rho Q^3 \sqrt{\varepsilon_0}}{I\sqrt{\sigma} d^4 \sqrt{L}} \tag{3.14a}$$

$$R_\mu = \frac{\mu Q^2 \sqrt{\varepsilon 0}}{I\sqrt{\sigma} d^2 \sqrt[3]{L^2}} \tag{3.14b}$$

$$R_\sigma = \frac{\sqrt{\sigma} Q \sqrt{\varepsilon_0}}{Id\sqrt{l}} \tag{3.14c}$$

Pairing these potential conditions resulted in six possible flows that are shown in Figure 5, where I, V, S, E and P define the regions of the flow and represent inertial, viscous, surface tension, electrostatic and polarization. Ganan-Calvo goes on to derive the current and jet diameter equations that result from asymptotic analysis. Additionally defined are the inertial and viscous coefficients (eq. 3.15 a, b) that are used to limit the range of validity for each of the equation sets.

Table 3-1. Summary of regimes of cone jet emission

Jet Region Dominace	Cone Necking Region	Current	Jet Diameter	Validity
Inertial (I)	Electrical Suction (E)	$I = \sqrt{\sigma K Q}$	$d = \sqrt[6]{\frac{\rho \varepsilon_0 Q^3}{\sigma K}}$	$\alpha_\rho >> \sqrt[4]{\alpha_\mu}$ $\frac{\alpha_\rho}{\beta - 1} >> 1$
Inertial (I)	Electrical Polarization (P)	$I = \sqrt{\frac{\rho K^2 Q^2}{(\beta - 1)\varepsilon_0}}$	$d = \sqrt[6]{\frac{\rho \varepsilon_0 Q^3}{\sigma K}}$	$1 >> \frac{\alpha_\rho}{\beta - 1} >> \frac{\alpha_\mu}{(\beta - 1)^4}$
Viscosity (V)	Electrical Suction (E)	$I = \sqrt{\sigma K Q}$	$d = \sqrt[8]{\frac{\mu \varepsilon_0^2 Q^3}{\sigma K^2}}$	$\alpha_\rho >> \sqrt[4]{\alpha_\mu}$ $\frac{\alpha_\rho}{(\beta - 1)^4} >> 1$
Viscosity (V)	Electrical Polarization (P)	$I = \sqrt{\frac{\mu^3 K^3 Q^3}{(\beta - 1)^4 \sigma^2 \varepsilon_0^2}}$	$d = \sqrt{\frac{\mu Q}{(\beta - 1)\sigma}}$	$1 << \frac{\alpha_\mu}{(\beta - 1)^4} << \frac{\alpha_\rho}{\beta - 1}$
Surface Tension (S)	Electrical Suction (E)	$I = \sqrt{\sigma K Q}$	$d = \sqrt{\frac{\varepsilon_0 Q}{K}}$	$\alpha_\mu \le 1$ $\alpha_\rho \le 1$ $(\beta - 1) \le 1$
Surface Tension (S)	Electrical Polarization (P)	$I = \sqrt{\frac{\sigma K Q}{\beta - 1}}$	$d = \sqrt{\frac{\varepsilon_0 Q}{K}}$	$\alpha_\mu \le (\beta - 1)^3$ $\alpha_\rho \le 1$ $(\beta - 1) > 1$

$$\alpha_\rho = \frac{\rho K Q}{\sigma \varepsilon_0} \tag{3.15a}$$

$$\alpha_\mu = \frac{K^2 \mu^3 Q}{\sigma^3 \varepsilon_0^2} \tag{3.15b}$$

The results of this analysis are quite striking when compared to existing findings of Fernandez de la Mora and Ganan-Calvo. First, in the case of flows dominated by inertial forces the jet diameter is defined by the same equation regardless of being suction or polarization dominate. This result for jet diameter is consistent with Ganan-Calvo earlier work. One of the over arching assumptions in the authors analysis was that a well defined cone would exist. However, in the areas where viscous dominate regime relations should hold no such clearly defined cone has been seen. This yields a question of validity of the relations in this region. Careful examination of the equations for surface tension and polarization dominate flow show that they match Fernandez de la Mora's equations quite closely. The only factor missing is f(ε) which if looked at in the context of this derivation would have to represent a correction for the relative polarity of the fluid. These base equations are only valid far from the boundaries defined by the range of validly and further adjustment would need to be done to make them truly valid for a particular fluid.

3.2.3. Startup Voltage Prediction. Taylor was able to produce a relation governing the necessary voltage to predict cone formation (eq. 3.16), where R_c is the radius of curvature near the tip [21]. Based on the balancing of electrostatic forces with the surface tension in the fluid this equation provides an estimate to required voltage only. One of the obvious factors missing in the equation is a finite back pressure from the pumping system.

$$V_{start} = \sqrt{\frac{\gamma R_c}{\varepsilon_0}} \ln\left(\frac{4d}{R_c}\right) \tag{3.16}$$

3.2.4. Validity of Existing Scaling Laws Application to Ionic Liquids. When examining the results of the scaling laws of Fernandez de la Mora, Chen and, Ganan-Calvo one is first struck by the differences in the functional form of f(ε) and G(ε). Despite using similar fluids the group's results showed drastically different behavior. Fernandez de la Mora's curve suggests a plateau in data while Chen and Ganan-Calvo show an ever increasing value. One possible solution suggested by Chen is that due to differences in the ion motilities the effective emitted current may have changed. Based on this only, one would expect very different f(ε) and G(ε) for ionic liquids because of the

complexity of ionic liquid ions and very different fundamental properties of the fluids. The general closed form solutions of Ganan-Calvo could be investigated for ionic liquid application by first determining the region in which the fluids would fall (i.e. IE, IP, VE, VP, SI SP). However, in its general form the equations do not match experimental results.

Due to the presents of ion evaporation the results for these scaling laws would become less reliable as the flow rate was decreased. Ultimately the equations cease to be accurate because of the increasing domination of ion evaporation compared to droplet emission. No theory currently presented in literature is capable of accurately predicting the PIR.

During the course of investigating the different models governing electrospray propulsion rather significant amounts of electrochemical data for 48 ionic liquids were gathered. These data which includes conductivity, melting temperature, viscosity, density, surface tension and dielectric constant have been tabulated and can be found in Appendix B. Reported values and errors are given with the corresponding reference from which they were obtained. In the case of single sources the value and error are reported as given in the reference. In the case of multiple sources the property value reported is the average of all sources and the error present is the standard deviation.

3.3. ESTIMATION OF ELECTROSPRAY PERFORMANCE

Fundamentally none of the current scaling laws have the ability to examine the mixed regime of ion emission and droplet formation much less the PIR. These equations are most applicable in the region of large drops. If PIR occurs, it is known to be manifested at very low flow rates. Predictions for the minimum flow rate η_{min} for solutions have varied from 0.5 to 1.4 and thus do not represent an exact prediction but perhaps a ball park value for experimentation. Predictions for the minimum flow rate for ionic liquids are currently not available. Similarly, the start up voltage is an approximation and does not represent an accurate solution. It was therefore necessary to approach the prediction of performance by other means.

3.3.1. Method of Performance Estimation. Although no formal method exists to determine whether an ionic liquid can produce a pure ionic regime, emission close to PIR has been reported for several ionic liquids [13, 22, 24, 25]. Generally, the fluid must

possess high conductivity and surface tension and a relatively low viscosity [23]. For all but the most viscous fluids, a regime close to PIR has been induced by heating the fluid [22]. This heating results in decreasing the fluid viscosity. The conductivity and viscosity of Fuel 1 (1.139 S/m and 0.0466 N/m respectively) show that it falls into the reported range of conductivity and surface tension of the other fluids reported to have obtained PIR [30, 31]. Unfortunately, electrochemical data for HAN and Fuels 2, 8, and 9 are unavailable in the published literature. Therefore, this work disregards the two ionic liquids based on 5-aminotetrazolate. It is important to note that if Fuel 2 could undergo PIR electrospray, its performance would be virtually identical to that of Fuel 1 because of their similar molecular composition. HAN is retained for further study because it represents a known ionic liquid monopropellant, and any resultant dual-mode system is of foremost interest. Because Fuel 1 has properties similar to those of ionic liquids that have shown PIR, it is assumed to operate in PIR with similar flow rates [13, 24, 30, 31].

Emission in the PIR consists of pure ions and ions traveling with clusters of N number of neutral pairs (degree of solvation). To calculate thrust and ISP, the percentage of the mass flow rate that is pure ions and ions of various degrees of solvation is required, and an approximate value is taken from previously published literature [13]. This percentage can be determined from time-of-flight curves for ionic liquids that have operated near PIR. Such time-of-flight curves were produced experimentally by grounding the voltage to the emitter and measuring the current emitted as a function of time. The ions arrive at the collector in order of least to greatest mass (higher solvation). Assuming an ideal collapse of emission; a typical curve would resemble that shown in Figure 3-2. The incremental reduction in current represents the final arrival time of a particular species. Assuming that all emission strikes the collector, this reduction also represents the steady current contribution of that species. Given the current contribution of a species, the mass flow rate of that species is given by equation 3.17, where m is the mass of one molecule of the species and e is the fundamental charge. The total mass flow rate of the jet would be found by summation of the component mass flow rates.

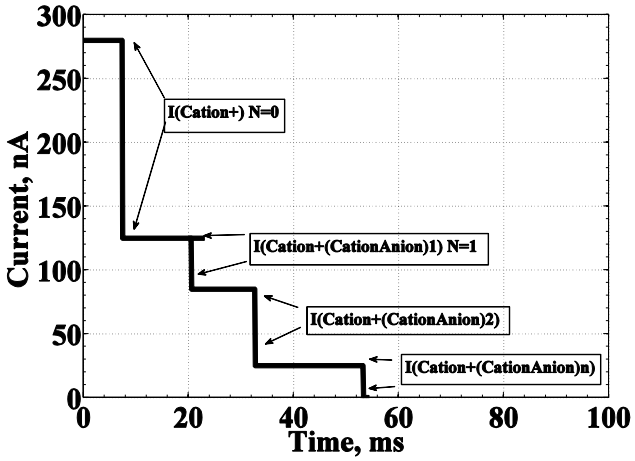

Figure 3-2: Idealized electrospray emission time flight curve

$$\dot{M}_i = \frac{I_i}{me} \tag{3.17}$$

Using this technique and actual time-of-flight curves, the average total mass flow rate for PIR emission ionic liquids is estimated as 1.2×10^{-12} g/s/emitter [32]. An examination of the curves[13] shows that, typically, only the first two ion states (N=0, 1) are present in the emission in any discernable quantity. The averaged result is a 40% emission of pure ions and a 60% emission of the first solvated state. In reality, the time-of-flight curve varies from the ideal because of collisions of molecules and nonfinite cessation of emission. Based on the available data; the potential associated with near-PIR emission for a typical ionic liquid is 1760 V [32].

3.3.2. Results of Analysis. The formulations of the equation governing the specific impulse of an electrospray are as follows. By definition the potential energy of a charge mass is given by the voltage times the charge. As the charged mass travels in the direction of decreasing potential it will trade this potential energy for kinetic energy. Thus, the final velocity of a charged mass in a potential field is given by equation 3.18. Since, the flow will consist of both pure ions and the first solvated state the effective ISP is given by equation 3.19; where V_A is the velocity of the pure ion and V_B is the velocity of first solvated state. R_A is the percent of the total mass flow rate that is pure ions.

Thrust is obtained by multiplying equation 3.19 by the total mass flow rate and the gravitation constant.

$$V = \sqrt{\frac{2e\Delta\phi}{MWAmu}} \tag{3.18}$$

$$Isp = \frac{V_A R_A + V_B(1 - R_A)}{g_0} \tag{3.19}$$

Applying the equations, the ISP for the system would be 6526s for HAN and 4511s for 1-butyl-3-methylimidazolium dicyanamide (BIMDCA). Using the power level and efficiency of the BHT-200 (200 W, 43.5%) produces a system thrust of 2.7 mN and 3.8 mN, respectively, for the propellants. A comparison of these results with the performance of the BHT-200 (1390 s, 12.8 mN) shows that thrust is traded for higher propellant efficiency when using an electrospray in PIR [33]. For HAN, if emitters of 50 μm inner diameter and 150 μm outer diameter were spaced 50 μm apart, the system would consist of 34,798 needles and occupy a circular area with a diameter of 5.3 cm. Comparison of this configuration with the space-charge-limit shows that the system would be operating at only 3-5% of the maximum.

4. DUAL-MODE BENEFITS TRADE STUDY

Three candidate dual-mode systems and two conventional systems are selected and investigated using the estimations for ionic liquid-based chemical and electric propulsion. Table 4-1 lists the performance specifications for these five systems. Performance values in terms of thrust and ISP were taken from sections 2 and 3 of this thesis for bipropellant and electrospray systems. Performance values for monopropellant and Hall thrusters were taken from literature [6, 33]. Systems 1 and 2 are typical on-orbit propulsion systems that use hydrazine and NTO in conjunction with a Hall thruster. The purpose of system 3 is to bridge the gap between completely conventional and pure dual-mode by using the same fuel in both chemical and electric modes, but using the conventional oxidizer NTO for chemical propulsion only. System 4 represents a pure dual-mode propulsion system that uses a combination of ionic liquid HAN and BIMDCA to accomplish both chemical and electric propulsion. A HAN monopropellant chemical thruster and electrospray thruster makes system 5 a dual-mode system. In the following sections, the performance of each of these systems is investigated using a realistic mass budget. The performance metric for each of these systems are maximum velocity change, time of flight, and mass consumption.

Table 4-1. Propulsion System Performance Specifications

System	1	2	3	4	5
Chemical Mode					
Propellant	N_2H_4	N_2H_4/NTO	BIMDCA/NTO	BIMDCA/HAN	HAN
ISP, s	227	270	239	267	218
Thrust, N	10	10	10	10	10
Mass Flow, g/s	4.4	3.7	4.2	3.7	4.6
Type	Monopropellant	Bipropellant	Bipropellant	Bipropellant	Monopropellant
Electric Mode					
Propellant	Xenon	Xenon	BIMDCA	BIMDCA/HAN	HAN
ISP, s	1390	1390	4511	5747	6526
Thrust, m N	12.8	12.8	3.8	3.4	2.7
Mass Flow, mg/s	0.94	0.94	0.09	0.06	0.04
Type	Hall	Hall	Electrospray	Electrospray	Electrospray

4.1. SYSTEM MASS BUDGET

For each of the five possible configurations of the spacecraft main propulsion system a mass budget is developed based on a 100 kg total spacecraft mass. In each case, a value of 35% of total system mass is devoted to the propulsion system. For each configuration, the subcomponent masses are determined based on literature data and an approximation methodology [20, 34, 35]. Such estimates are necessary because the amount of fuel available for each system varies based on the mass of its support hardware. For the conventional systems, total system mass is divided evenly between electric and chemical propulsion subsystems.

Representative values (in the range of performance being investigated) for the mass of monopropellant, bipropellant, and Hall thrusters are obtained from literature [20, 34, 35]. Monopropellant and bipropellant thrusters have an average mass of 0.21 kg and 0.54 kg respectively, with standard deviations of 0.09 kg and 0.18 kg. To ensure conservative estimates, monopropellant and bipropellant thruster mass is estimated as 0.3 kg and 0.7 kg. Available literature did not indicate the mass of a BHT 200 Hall thruster, but the similarly sized SPT-50 has a mass of 0.8 kg [36]. Since the electrospray thruster is essentially a crucible with a lid consisting of emitters and an extraction grid, the mass is assumed to be at least half that of the Hall thruster. Data in literature also provides the mass of the power processing unit (PPU) for both types of electric propulsion [37, 38]. Based on values reported for NSTAR, NEXT, and SPT-50 PPU, the specific power is 161 W/kg, resulting in a PPU mass of 1.3 kg for these systems.

Each main propulsion system also contains propellant tanks, pressurization tanks, feed lines, regulation valves, and mounting brackets. The masses of these subcomponents are determined using methodologies described by Humble, Henry, and Larson [39]. The propellant tank pressures are determined by starting with the specified chamber pressure of 300 psi and backing up through the propellant feed system. An injector head loss of 20% of the chamber pressure is assumed, along with overall line losses of 0.35 psi. The mass of each chemical propellant tank is calculated from the propellant storage pressure, the propellant volume (assuming a liquid incompressible state), and material properties. The mass of the Hall thruster xenon propellant tank was computed assuming a maximum

pressure of 1450 psi using equation 4.2. Because of the high pressure, the volume of xenon was evaluated using the Van der Waals equation of state in place of the ideal gas law [40].

$$M_{ct} = 6\frac{M_p \rho_m P_t}{\rho_P F_{tu}} \tag{4.1}$$

$$M_{et} = 6\frac{V_{xe} \rho_m P_t}{F_{tu}} \tag{4.2}$$

A pumping system is required to maintain a constant propellant flow rate, (due to the low mass of the system) and a pressure feed system is selected. Such a system must provide enough pressurant to occupy the volume of the entire main propulsion system at a pressure at least equal to the tank pressure. The pressurant tank pressure is limited to 1450 psi so that it is typical of spacecraft pressure vessels. When the pressure is limited, the mass of pressurant gas becomes coupled with the volume of the pressurant tank itself. Thus, an iterative procedure is used to compute both the mass of pressurant gas and the volume of the pressurant tank. The mass of the pressurant required to fill the main propulsion system is computed for an initial volume equal to that of the propellant tanks. The volume needed to store the pressurant is then computed. This new volume is added to the initial volume, and the total volume is used to calculate a new pressurant mass. This process is repeated until convergence, providing both pressurant mass and pressurization tank volume, and thus the pressurant tank mass.

The mass of lines and regulation valves are provided by the CPIA manual [20]. For typical monopropellant and bipropellant systems at the thrust level under consideration here, the mass of lines and valves combined would be approximately 50% and 90% of the thruster mass, respectively. Due to the high disparity between storage pressure and thruster pressure in electric propulsion systems, the valves and lines for the Hall thruster are assumed to have the same percent mass as those for the bipropellant thrusters. This value of 90% of the thruster mass is also assumed for the electrospray

thruster because of the need for a high degree of mass flow control. Based on methods in literature, mounting brackets are assumed to be 10% of the total mass of the other components in the system [39]. Since the total mass of the main propulsion system is limited to 35 kg, all of these approximations are used in an iterative routine to find the distribution of system mass among the components. Table 4-2 shows the results of this analysis.

Table 4-2. Mass budget break down for all systems

System	1	2	3	4	5
Thruster, kg	1.10	1.50	1.10	1.10	0.70
Fuel, kg	14.06	7.31	14.27	14.87	27.71
Oxidizer, kg	0.00	6.10	11.89	11.44	0.00
Pressurant, kg	0.60	0.50	0.94	0.88	0.67
Fuel Tank, kg	0.37	0.19	0.38	0.37	0.41
Oxidizer Tank, kg	0.00	0.11	0.22	0.17	0.00
Pressurant Tank, kg	0.47	0.39	0.74	0.70	0.53
Lines/Valves, kg	0.87	1.35	0.99	0.99	0.51
Xenon, kg	12.25	12.25	0.00	0.00	0.00
Xenon Tank, kg	0.82	0.82	0.00	0.00	0.00
PPU, kg	1.33	1.33	1.33	1.33	1.33
Structural Mounts, kg	3.19	3.19	3.19	3.19	3.19

4.2. MEASURE OF SYSTEM PERFORMANCE

Measures of propulsion performance in the dual-mode systems are based on the total change in velocity, the mass of propellant consumed, and the time required to produce the velocity change. All orbital perturbations are disregarded, as are potential

gravity losses inherent in low-thrust applications. Therefore, the change in velocity reported here is ideal. Each of these metrics is computed as a function of the fraction of the total velocity change that is accomplished by electric propulsion; this is referred to as the EP fraction. For example a value of 0 EP means that all change in velocity is accomplished by chemical means only. Whereas 1 EP would mean that all change in velocity is accomplished by electric means.

To determine the total velocity change each system could produce, the rocket equation was used in a two-part form (equation 4.3) were c_{chem} and c_{elec} are the exhaust velocities, and the first term represents the change in velocity provided by chemical means and term two that provided by electric means. The values of satellite mass at the end of each subsequent burn (m_{f1} chemical thrust and m_{f2} electric thrust) were restricted based on the available propellant masses as described in section IV A above. Further, all chemical thrusting was assumed to take place before the electric thrusting. To determine the time required to apply the change in velocity, the mass flow rate of each thruster type was used in conjunction with the total mass of propellant consumed. The result is the sum of the chemical burn time and electric thrust time (eq. 4.4).

$$\Delta V = c_{chem} \ln\left(m_0 / m_{f1} \right) + c_{elec} \ln\left(m_{f1} / m_{f2} \right) \tag{4.3}$$

$$t = c_{chem} \frac{(m_0 - m_{f1})}{T_{chem}} + c_{elec} \frac{(m_{f1} - m_{f2})}{T_{elec}} \tag{4.4}$$

4.3. RESULTS OF TRADE STUDY

Figure 4-1 shows the results for system 1. This is the hydrazine monopropellant Hall thruster configuration. Figure 4-1a shows the fraction of hydrazine (N2H4) consumed as a function of the change in spacecraft velocity for different values of EP fraction. At 0 EP, a maximum velocity change of 370 m/s is obtained, and all of hydrazine propellant mass is consumed. At 0.86 EP the maximum velocity of the system transitions from being limited by chemical propellant to being limited by electric propellant. Increasing the EP fraction beyond this point leaves unused chemical

propellant in the tank, thus incurring a mass penalty for accelerating the chemical propellant; if the fuel is not burned, the potential change in velocity is not realized. For example, in Figure 4-1a, operating at 0.95 EP achieves higher change in velocity than at an EP fraction of 1. For the 0.95 EP case 30% of hydrazine was used were at 1 EP all of the hydrazine propellant remains. Thus, at 0.95 EP the spacecraft has less mass to accelerate when the electric mode is used. Operating with an EP fraction of 1 would result in no consumption of hydrazine fuel. Chemical propellant remains in the tank after 0.86 EP because there is insufficient xenon to produce a higher change in velocity. In the region from 0.86 EP to 1 EP xenon is the limiting factor in change in velocity.

Figure 4-1b shows the fraction of xenon propellant consumed as a function of the change in spacecraft velocity for different values of EP faction, these results correspond with Figure 4-1a. At 0 EP, no xenon propellant is consumed. As the EP fraction increases the fraction of xenon propellant consumed raises. At an EP fraction of 1 the maximum velocity obtained is 1780 m/s, this is however not the maximum velocity that the system can produce. The maximum velocity of 2249 m/s occurs at the point of transition 0.86 EP. For values of EP lower than 0.86 the chemical propellant is the limiting factor in change in velocity and xenon will remain in the tank.

Figure 4-1c shows the time required to obtain a specific change in velocity for different values of EP fraction. At 0 EP the time required to accomplish the maximum change in velocity is only 52 minutes. As the EP fraction is increased the time required to perform the change in velocity increases until it reaches 150 days. The maximum velocity change also takes approximately 150 days.

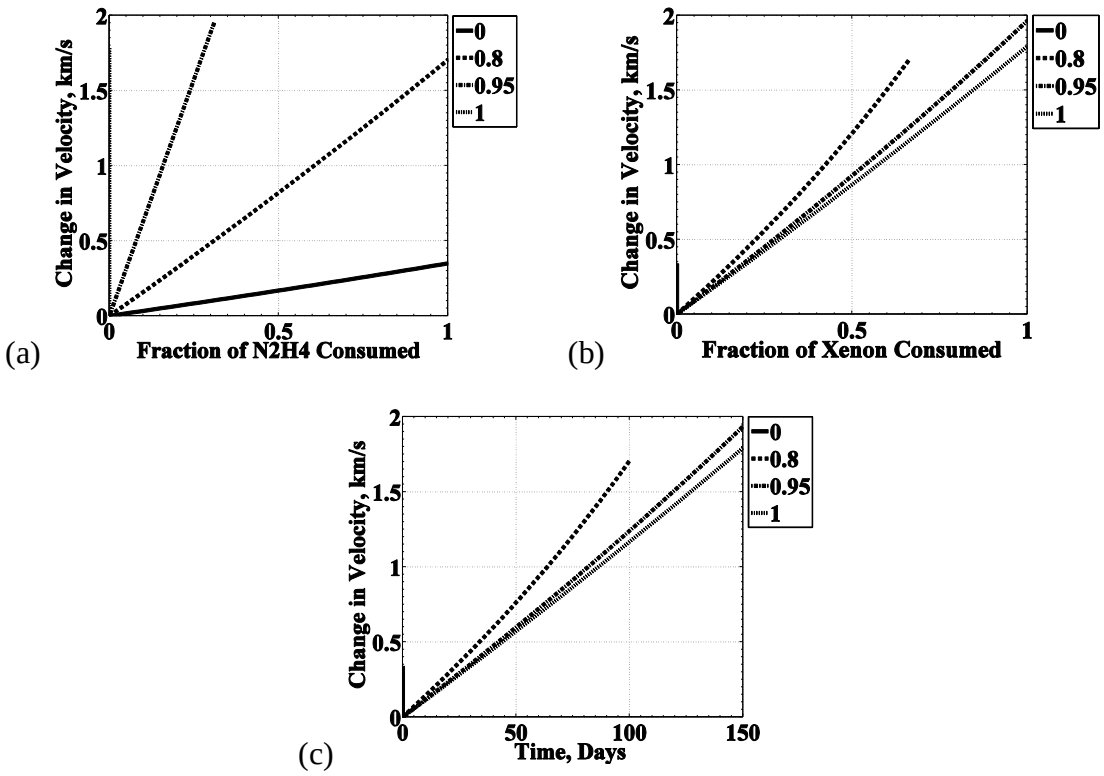

Figure 4-1: System 1 Monopropellant N2H4 Hall Thruster performance
(a) N2H4 consumption versus change in velocity and EP fraction
(b) Xenon consumption versus change in velocity and EP fraction
(c) Time required to execute change in velocity versus EP fraction

Figure 4-2 shows the performance of system 2. In this case hydrazine is used in a bipropellant system paired with NTO and a Hall thruster is used for electric propulsion. By using a bipropellant thruster a change in velocity of 400 m/s is possible at 0 EP. Figure 4-2a, b show that this results in the complete consumption of both the hydrazine and NTO propellants. As the fraction of EP is increased, the fraction of NTO and hydrazine consumed are identical because they are directly related through the equivalence ratio. The same transition from chemical propellant limited to electric propellant limited observed in system 1 occurs for system 2; in the case of system 2 it occurs at 0.85 EP. At this point the maximum velocity is 2460 m/s. Because of the increased dry mass of system 2, it produces only a 2% greater change in velocity despite

having an ISP 19% greater than system 1. The Hall thruster is burdened by the extra dry mass of the bipropellant system resulting in a decrease in system acceleration. As with the case of system 1, any increase in the EP fraction will result in higher xenon consumption (Figure 4-2c). A decrease in chemical propellant consumption only occurs after the transition point. Figure 4-2d shows that at 0 EP, system 2 requires 59 minutes for maximum change in velocity. As with all systems, an increase in EP fraction results in longer thrust duration. Similar to system 1, performing maximum change in velocity at the transition point requires 150 days.

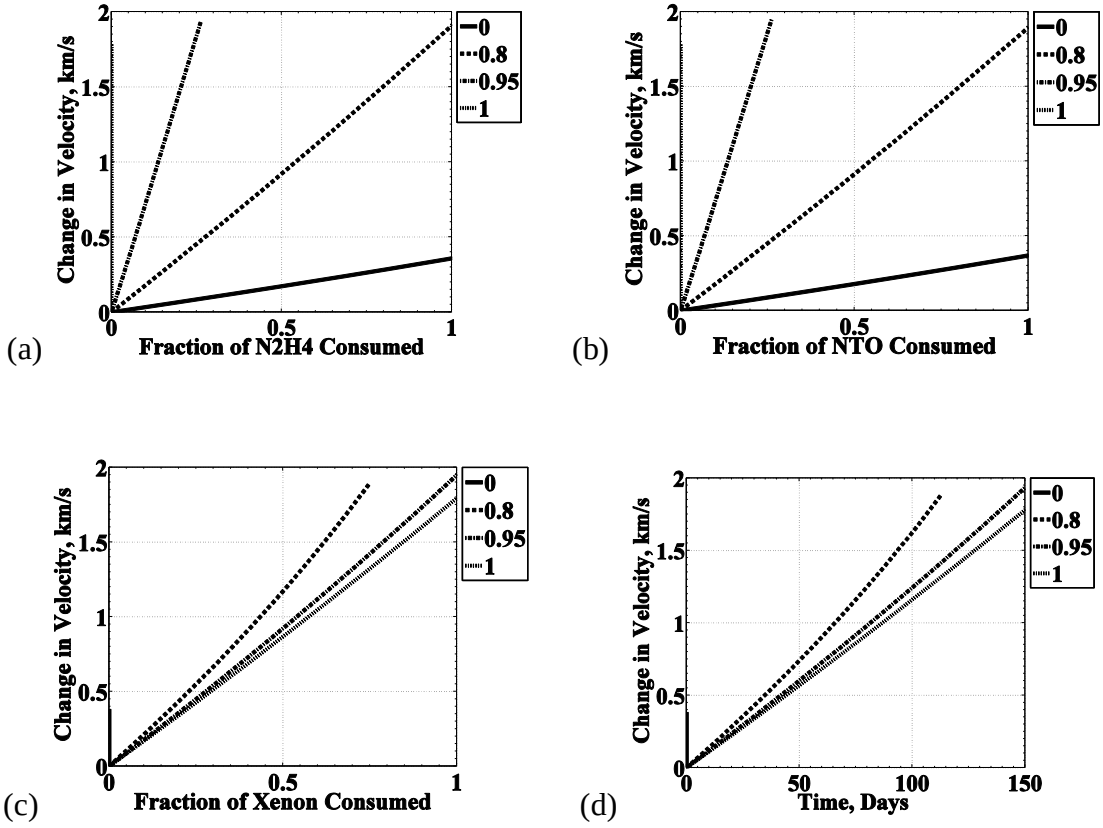

Figure 4-2: System 2 Bipropellant N2H4 NTO Hall Thruster Performance
(a) N2H4 consumption versus change in velocity and EP fraction
(b) NTO consumption versus change in velocity and EP fraction
(c) Xenon consumption versus change in velocity and EP fraction
(d) Time required to execute change in velocity versus EP fraction

Figure 4-3 shows the performance of system 3. In this system the ionic liquid BIMDCA is substituted for hydrazine in the bipropellant thruster, NTO is maintained as the oxidizer. In place of a Hall thruster an electrospray thruster is used, also operating on BIMDCA. At 0 EP system 3 is capable of producing a velocity change of 711 m/s. This velocity change is greater than in the case of system 2 despite having lower ISP. Greater velocity change is possible because more propellant mass is available since system 3 is partially a dual-mode system. System 3 obtains a maximum velocity change of 6813 m/s at an EP fraction of 1. Figure 4-3a shows at all EP fractions all of the BIMDCA is consumed. However, as EP fraction increases, greater amounts of the NTO remain unused until at an EP fraction of 1 all of the NTO remains in the tank (Figure 4-3b). The extra oxidizer mass decreases performance, and is probably best ventilated in proportion to the amount of BIMDCA consumed. Ventilation of the NTO would leave the system capable of performing the maximum chemical change in velocity, while increasing the electric propulsion performance because of the reduced system mass. The penalty is that the oxidizer is put into orbit with the spacecraft and now provides no gain to overall system performance (Figure 4-3c). At 0 EP, 102 minutes are required to perform the maximum velocity change. At an EP fraction of 1, 1624 days are required to produce maximum change in velocity.

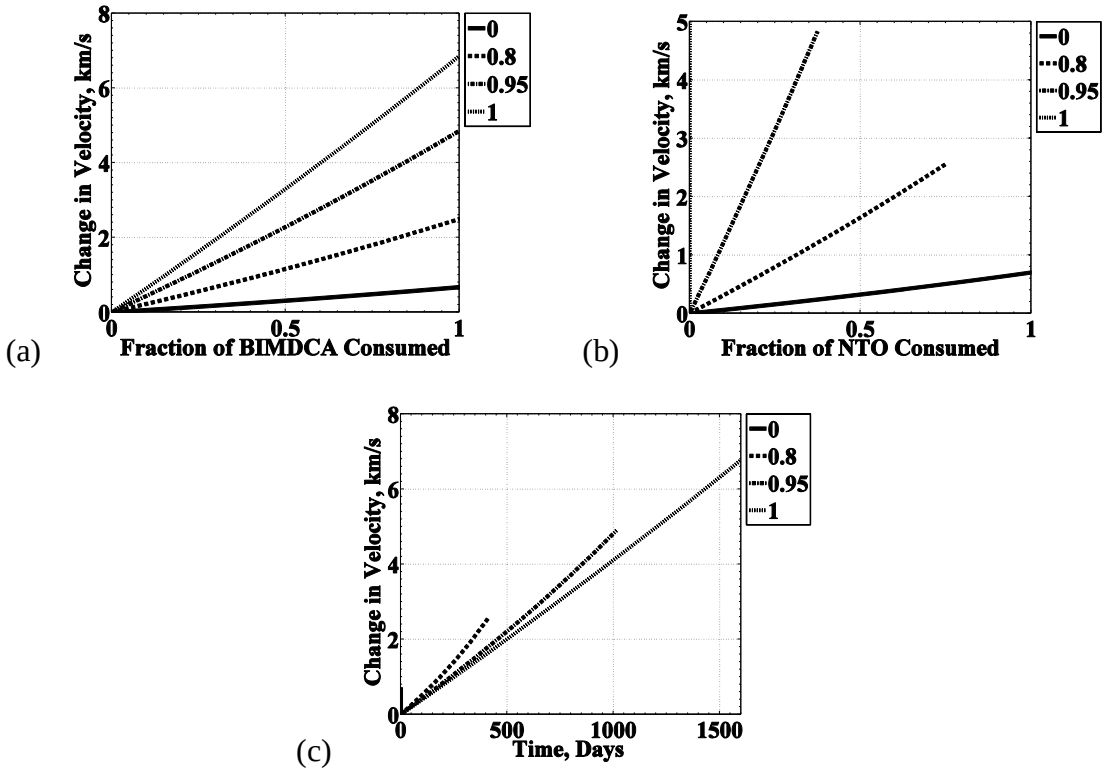

Figure 4-3: System 3 BIMDCA NTO Bipropellant Electrospray Performance
(a) BIMDCA consumption versus change in velocity and EP fraction
(b) NTO consumption versus change in velocity and EP fraction
(c) Time required to execute change in velocity versus EP fraction

Figure 4-4 shows the performance of system 4. For system 4 BIMDCA is retained as the bipropellant fuel, but the oxidizer HAN is used in place of NTO. At 0 EP the maximum velocity change possible is 808 m/s, all of the BIMDCA and HAN propellants are consumed (Figure 4-4a, b). For all EP fractions all propellants are consumed. By augmenting the electrospray of BIMDCA with higher ISP HAN, a maximum velocity of 17210 m/s is obtained for an EP fraction of 1. Figure 4-4c shows as with all systems, that an increase in EP fraction results in longer thrust duration. At 0 EP, 116 minutes is required for maximum velocity change. This increases to 13.8 years for the case of 1 EP.

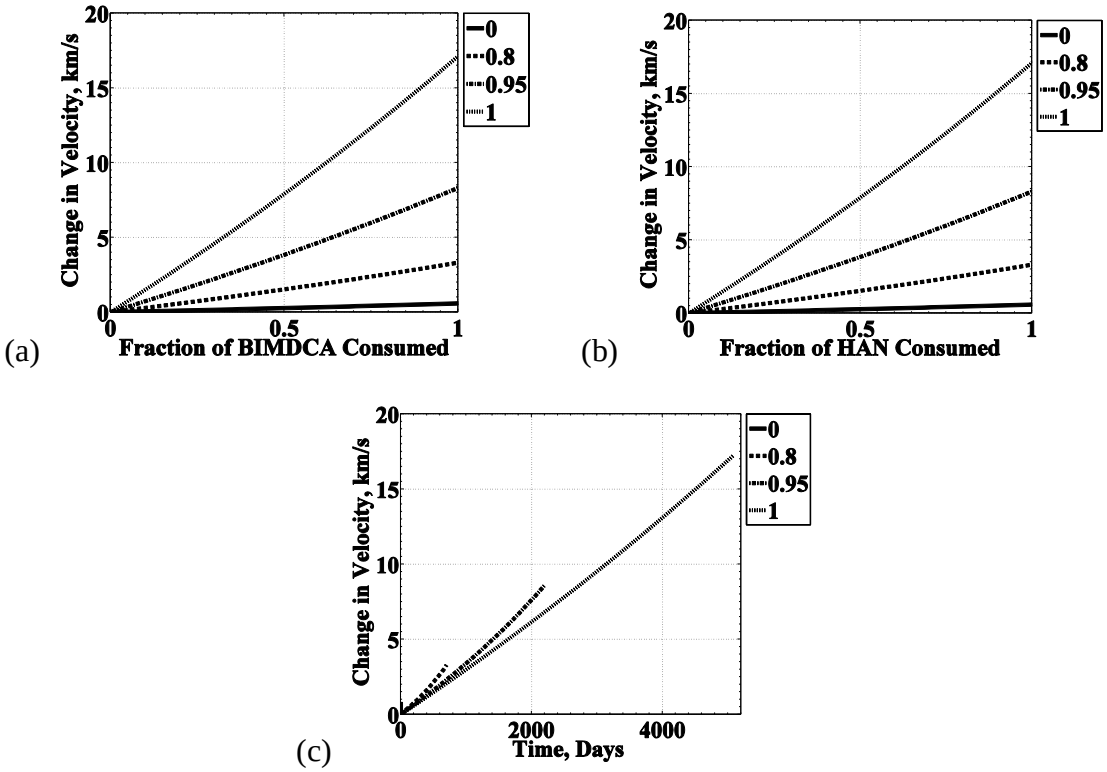

Figure 4-4: System 4 Bipropellant BIMDCA HAN Electrospray Performance
(a) BIMDCA consumption versus change in velocity and EP fraction
(b) HAN consumption versus change in velocity and EP fraction
(c) Time required to execute change in velocity versus EP fraction

Figure 4-5 shows the results for system 5. This is the HAN monopropellant and electrospray configuration. Figure 4-5a shows the fraction of HAN consumed as a function of the change in spacecraft velocity for different values of EP fraction. At 0 EP the maximum velocity achieved is 630 m/s. At this point all of HAN propellant is consumed. Notice that unlike in the case of system 1 only one chart describes consumption of propellant in case of system 5 because of the use of a common propellant between electric and chemical modes. Increasing the fraction of EP will not change the amount of propellant consumed, for any dual-mode system no matter the fraction of EP all of the propellant will be consumed. The maximum velocity for system 5 is 20700 m/s and occurs at an EP fraction of 1. The use of the common propellant means no point of transition exists as in the case system 1. Instead, the maximum velocity for any system

using dual-mode occurs when the propellant is being used completely as an electric propellant.

Figure 4-5b shows the time required to obtain a specific change in velocity for different values of EP fraction. At 0 EP the time required to perform the velocity change is only 99 minutes. This is nearly twice the time required by system 1 because both systems have a thrust of 10 N, but system 5 has nearly twice the available chemical propellant as system one by using a common propellant. Because the system 5 electrospray thruster has an ISP 4.7 times greater than that of system 1, it requires 21 years to accomplish the maximum change in velocity.

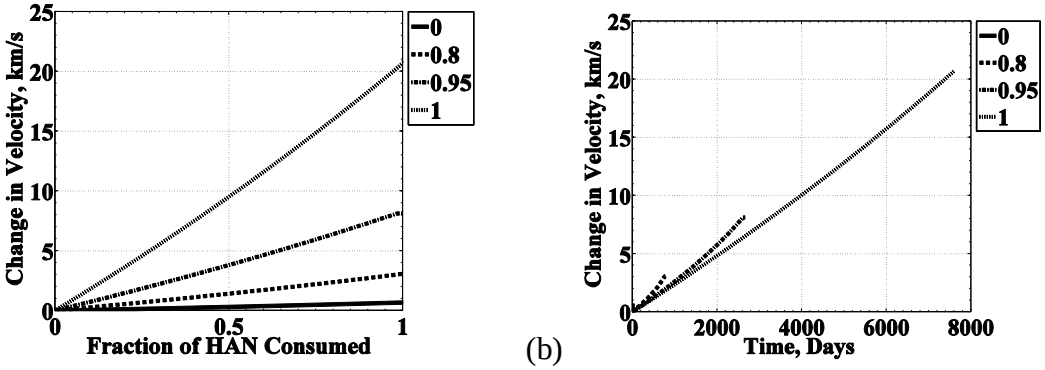

Figure 4-5: System 5 Monopropellant HAN Electrospray Performance
(a) HAN consumption versus change in velocity and EP fraction
(b) Time required to execute change in velocity versus EP fraction

4.4. TRADE STUDY ANALYSIS

Figure 4-6 presents a comparison of maximum change in velocity for all five systems. It is evident that the performance of systems 1 and 2 are virtually identical for small changes in velocity, with a small advantage for system 2 at higher EP fraction. The performance of systems 1 and 2 become effectively identical once the xenon propellant becomes the limiting factor in maximum velocity change for both systems (occurring at 0.86 EP and 0.85 EP, respectively). Initially, both bipropellant systems 3 and 4 outperform the monopropellant system 5 in maximum velocity change. This is expected

because of the increase in chemical ISP performance for the bipropellant systems. The ISP performance of system 5 overtakes that of system 3 at 0.37 EP. System 5 does not surpass the performance of system 4 until it reaches above 0.95 EP. Sharing common propellants between the chemical and electric modes allows for an overall larger change in velocity due to the greater availability of propellant. Due to the higher ISP present in the electrospray systems and the greater availability of propellant, the maximum change in velocity increases by an order of magnitude for the dual-mode systems compared to systems 1 and 2.

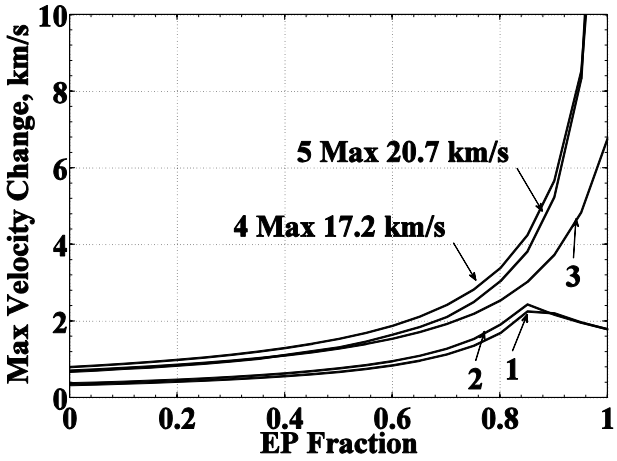

Figure 4-6: Maximum velocity change versus EP fraction for systems 1-5

Figure 4-7 shows the total propellant expended for the maximum change in velocity shown in Figure 4-6. Examination of systems 4 and 5 in Figure 4-7 shows that a dual-mode system offers the advantage that under any thrusting condition all propellant is consumed. Comparing Figure 4-1 and Figure 4-5 shows that systems 4 and 5 consume the most propellant but also produce the highest change velocity. Sharing common propellants has permitted systems 4 and 5 to have the greatest propellant masses. System 3 initially consumes all of the BIMDCA and NTO propellants but as the EP

fraction is increased the amount consumed decreases because of the residual NTO oxidizer. Starting at around 0.75 EP, systems 1 and 2 show an interesting exchange in propellant mass consumed. At this point, the bipropellant system 2 consumes more propellant than system 1 because of the larger amount of chemical propellant present in system 1. At each EP fraction until the systems reach their respective transition points, all chemical propellant is expended. As a result, when system 2 begins its electric thrusting it has a higher dry mass to accelerate. This extra mass requires additional xenon propellant to affect the EP fraction of the total change in velocity, thus resulting in higher propellant use. Also, at each EP fraction the bipropellant system is producing higher change in velocity therefore the xenon Hall thruster is required to perform a higher change in velocity to maintain the EP fraction, resulting in higher propellant consumption.

This effect ceases almost immediately after the xenon propellant becomes the limiting factor in the maximum velocity. In the region from an EP fraction of 0.85 to 1, system 1 consumes more propellant mass than system 2 because now less of the chemical propellant is consumed. This leaves additional mass for the electric propulsion system to accelerate, resulting in a higher consumption of xenon and thus, a higher total propellant mass. Additionally the higher EP fraction dictates that the Hall thruster is limiting factor in total change in velocity. Therefore less bipropellant fuel is consumed to effect the same change in velocity as the monopropellant system. Significantly Figure 4-6 demonstrates that at no point during this transition does system 1 affect a greater change in velocity than system 2. System 3 shows a gradual decline in propellant consumed as the EP fraction increases. At EP of 1, the total initial mass of the NTO oxidizer remains. For example, if system 1 and 5 are operated at 0.8 EP fraction, system 1 requires 100 days to produce a 1.7 km/s change in velocity. Whereas system 5 requires 2300 days to produce an 8 km/s change in velocity.

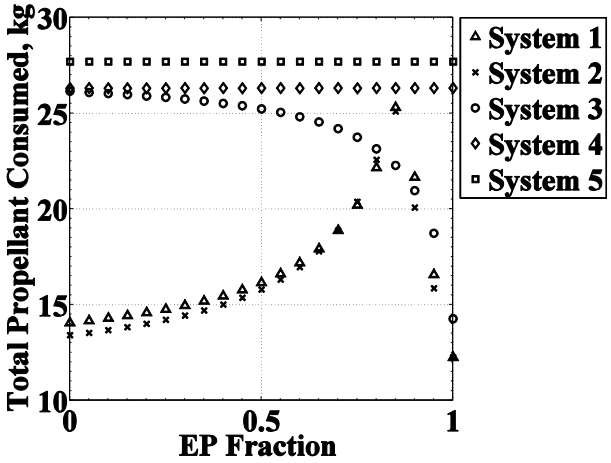

Figure 4-7: Total propellant consumed versus EP fraction for max change in velocity

Figure 4-8 shows that the improved propellant savings associated with higher EP fraction comes at the cost of mission time. Maneuvers taking hundreds, or in the case of the electrospray systems thousands of days are required to reach maximum change in velocity. In the case of conventional systems, a plateau in mission time is observed because once the maximum change in velocity is reached for both systems, the systems are already thrusting for as long as possible. After this point, the few hours required to fire the chemical systems are insignificant in comparison to the 150 days to expel the xenon propellant, resulting in the effective plateau.

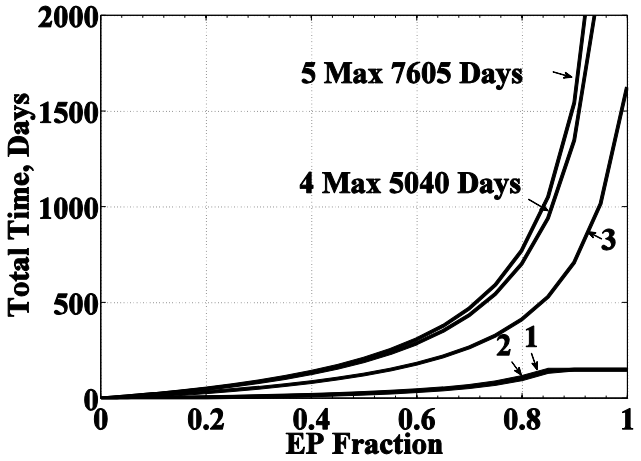

Figure 4-8: Total time required for maximum change in velocity versus EP fraction for systems 1-5

Because of the use of common propellants, the dual-mode systems are able to perform greater velocity changes than the conventional analogs at the cost of higher thrust durations. Examination of Figure 4-6 and Figure 4-8 shows that for an EP fraction of 0.8, system 5 produces a maximum of 3.03 km/s change in velocity in 750 days. For same value of EP fraction system 1 produces a maximum of 1.6 km/s in 100 days. Using system 5 at 0.85 EP trades 750% more thrust time to produce a 190% increase in change in velocity. Figure 5b shows that systems 5 requires 470 days or 470% more time to match the maximum change velocity achieved by system 1 operating at 0.8 EP.

Given that the mass budget for the traditional systems is based on even distribution of system mass between the electric and chemical systems one might imagine the case of a pure bipropellant chemical system operating with same total system mass. The result would be that a slight advantage in total chemical change velocity would go to the traditional system because of its superior ISP and the additional propellant mass it obtains by not supporting the electric system dry mass. However, the dual-mode system would have the ability to outperform the traditional system assuming time-of-flight is not the primary consideration.

5. CONCLUSION

A class of propellants known as ionic liquids are identified that can be used in both chemical and electric modes of propulsion. In terms of specific impulse, the performance of the ionic liquids are comparable to existing space storable propellants hydrazine and NTO, with only a 3-12% reduction in ISP when the ionic liquids were paired with NTO. If the ionic liquids are combined with HAN this performance gap reduces to 0-4% when compared with hydrazine/NTO combination. Ionic liquid HAN produces greater specific impulse than NTO when combined with any of the fuels investigated. Density impulse is found to be up to 40% greater than traditional propellants because of the larger density of ionic liquids. Based on the ionic liquids examined the long term storability of such fluids may be in question as most of propellants would require extensive heating to maintain a liquid state. Overall, the performance results with HAN as an oxidizer warrant further experimental investigation despite not being considered a storable propellant. An extensive investigation of ionic liquids thermodynamic properties needs to be under taken as these results are only for a few select ionic liquids out of hundreds available for study.

When operated in an electrospray, (given the same input power) ionic liquids may offer up to 4.5 the specific impulse the traditional Hall Effect thruster by operating in a regime of nearly pure ionic emission. The assumption of purely ionic emission means that values of ISP determined represent an upper bound in possible electrospray performance. In future systems, the ISP of electrospray thrusters may be decreased by forcing the system to operate in the droplet emission mode. This approach may effectively trade propellant efficiency for higher thrust. Thus, in terms of ISP, the dual-mode systems may match the performance of a range of systems from low-performance monopropellant systems to the level of state-of-the-art electric propulsion systems. This flexibility in performance may offer the major advantage of adaptability to new missions. However, the ability to accurately predict the performance of such systems needs to be investigated if practical high performance systems are to be developed. This will also require the extensive investigation of electrochemical properties of conductivity, viscosity, surface tension, and dielectric constant.

Three potential dual-mode systems are modeled here based on the performance predicted for chemical and electric propulsion for ionic liquids, and are compared to two conventional propulsion systems. Because of the common propellants, the dual-mode systems are able to perform greater velocity changes than the conventional analogs at the cost of higher thrust durations. Specifically, if 80% of the velocity change is accomplished by using electric propulsion, a HAN monopropellant electrospray system produces 190% more change in velocity than a traditional system consisting of a hydrazine monopropellant and a xenon Hall effect thruster. This 190% increase in maximum velocity change comes at the cost of 750% more time thrusting for the HAN system.

The use of a dual-mode system offers numerous mission benefits resulting primarily from its flexible thrust history. The growing threat of orbit debris offers a great opportunity for dual-mode systems. Their flexibility may permit an asset to respond quickly to an imminent hazard using a primarily chemical maneuver and slowly return to its original orbit using higher efficiency electric propulsion as the potential threat subsides. On the other hand, if no threat is encountered, the system may provide long-term orbit maintenance capability. In the fast-paced world of military conflict, such systems are ideal for rapid deployment of space assets. With little knowledge of the thrust history prior to deployment, a generic spacecraft may have a thrust history that is dictated as the mission evolves, rather than prior to launch. The concepts of orbital refueling and space tugs may also benefit from a dual-mode propulsion system, sharing a common propellant means both the tug and the assets being transported (or refueled) will operate on the same propellant.

A dual-mode space propulsion system has been shown to be plausible and that the in terms mission flexibility and total change in velocity it will have a significant advantage over conventional systems. The use of ionic liquids represents only one possible configuration by which a dual-mode system could be produced, other system configurations are possible and should also be investigated. The concept of dual-mode spacecraft propulsion in any form would represent a substantial step forward in technology and should be pursued.

APPENDIX A.
DETAILED CHEMICAL PERFORMANCE CHARTS

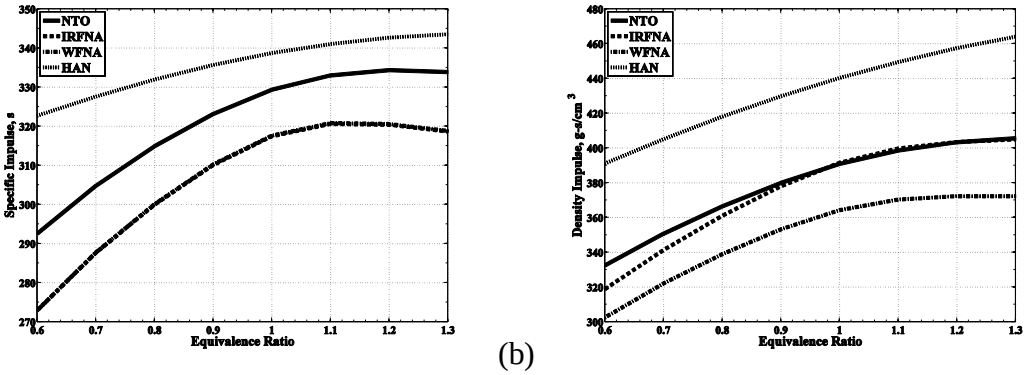

Figure A-1: Hydrazine combined with select oxidizers versus equivalence ratio
(a) Performance measured in specific impulse
(b) Performance measured in density impulse

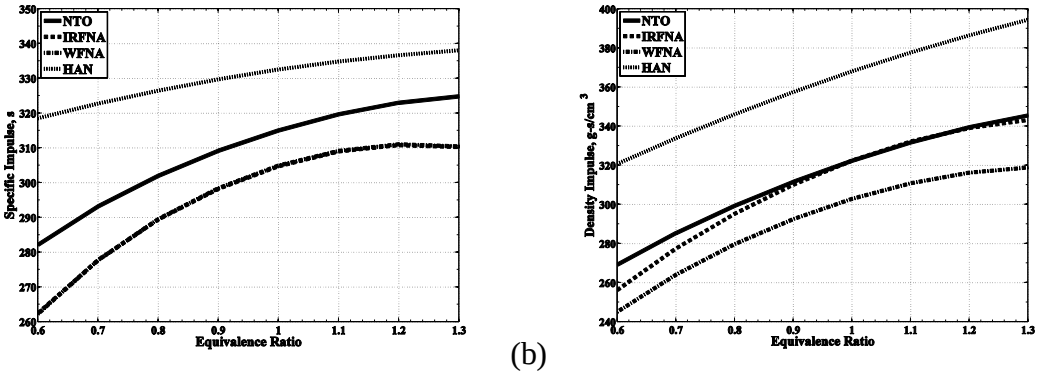

Figure A-2: UDMH combined with select oxidizers versus equivalence ratio
(a) Performance measured in specific impulse
(b) Performance measured in density impulse

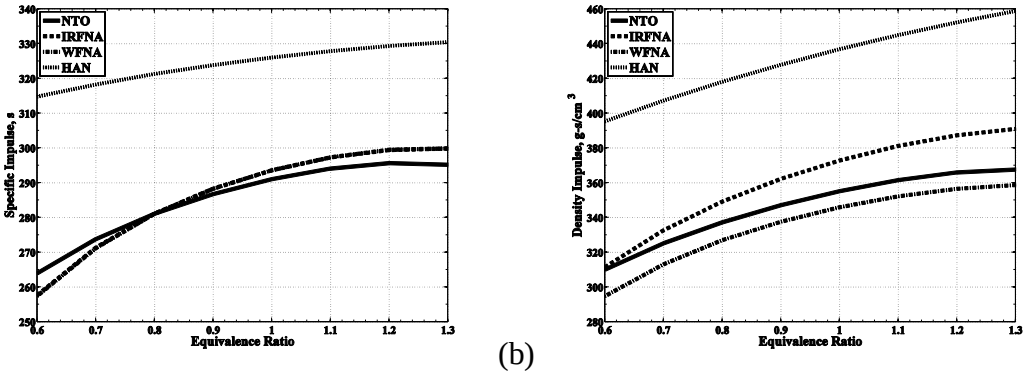

Figure A-3: Fuel 1 $C_{10}H_{15}N_5$ combined with select oxidizers versus equivalence ratio
(a) Performance measured in specific impulse
(b) Performance measured in density impulse

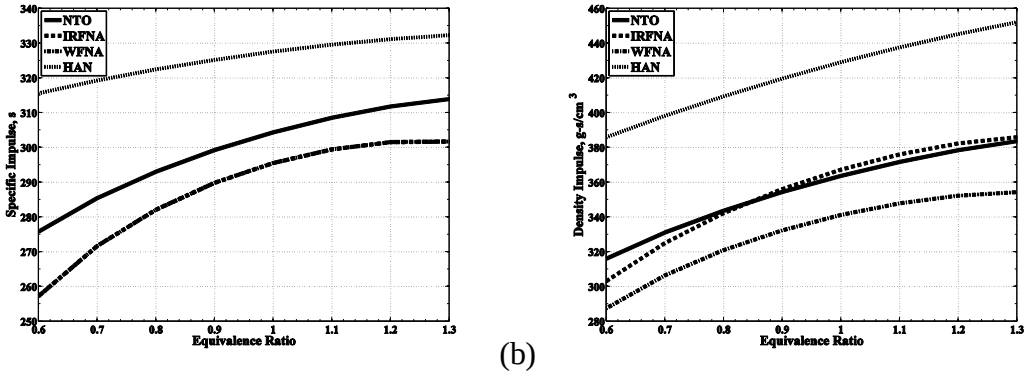

Figure A-4: Fuel 2 $C_{11}H_{20}N_4$ combined with select oxidizers versus equivalence ratio
(a) Performance measured in specific impulse
(b) Performance measured in density impulse

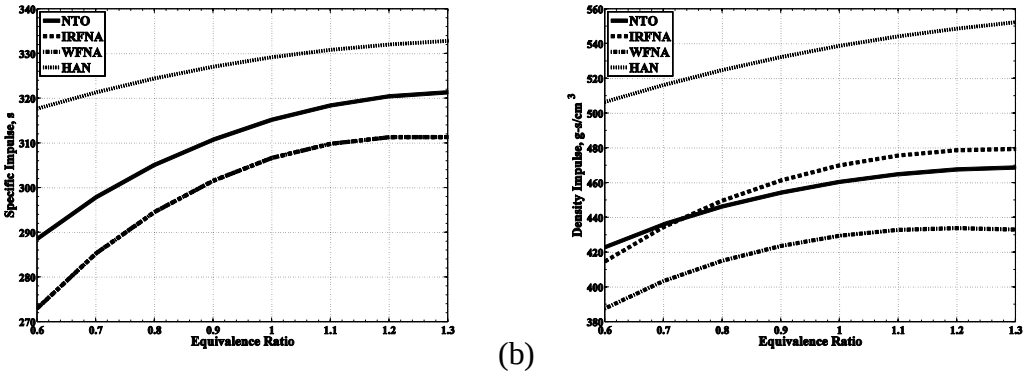

Figure A-5: Fuel 3 CH_7N_7 combined with select oxidizers versus equivalence ratio
(a) Performance measured in specific impulse
(b) Performance measured in density impulse

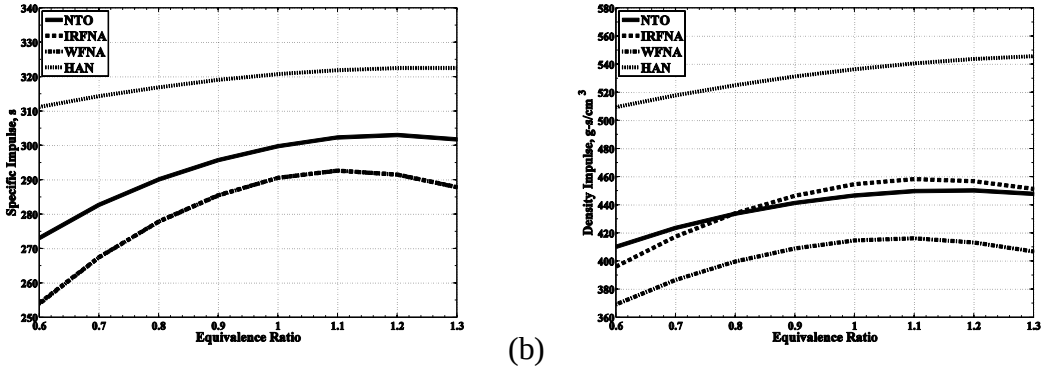

Figure A-6: Fuel 4 $C_2H_8N_8$ combined with select oxidizers versus equivalence ratio
(a) Performance measured in specific impulse
(b) Performance measured in density impulse

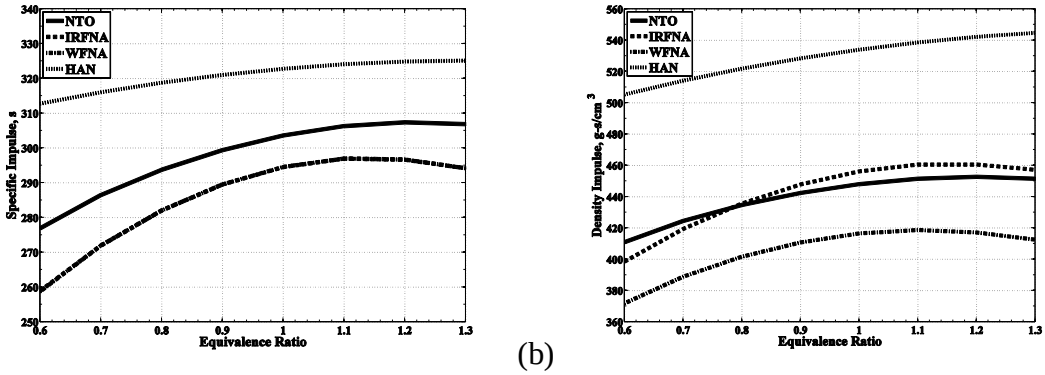

(a) (b)

Figure A-7: Fuel 5 $C_2H_9N_9$ combined with select oxidizers versus equivalence ratio
(a) Performance measured in specific impulse
(b) Performance measured in density impulse

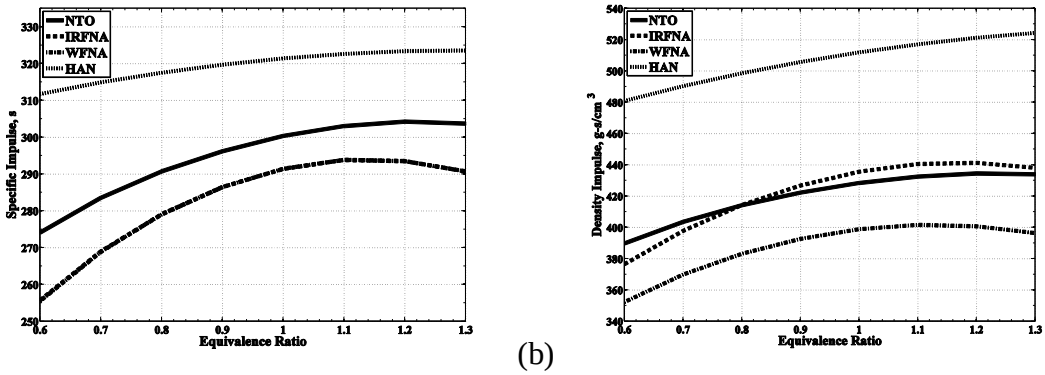

(a) (b)

Figure A-8: Fuel 6 $C_3H_{10}N_{10}$ combined with select oxidizers versus equivalence ratio
(a) Performance measured in specific impulse
(b) Performance measured in density impulse

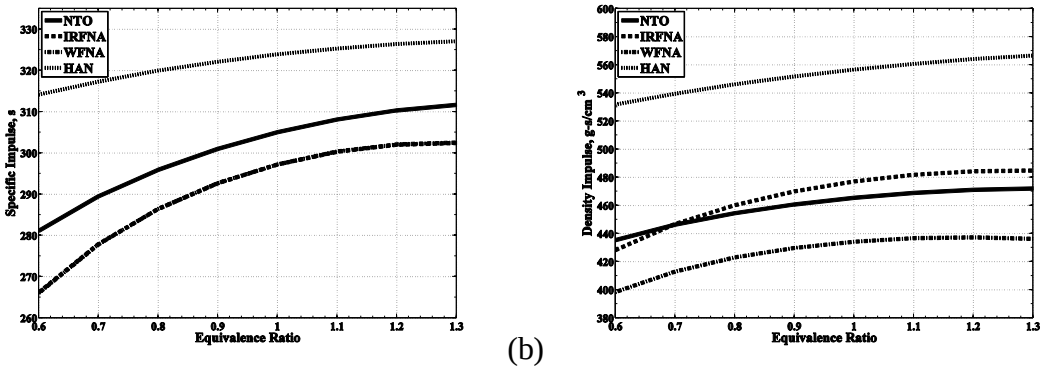

Figure A-9: Fuel 7 $C_3H_7N_9$ combined with select oxidizers versus equivalence ratio
(a) Performance measured in specific impulse
(b) Performance measured in density impulse

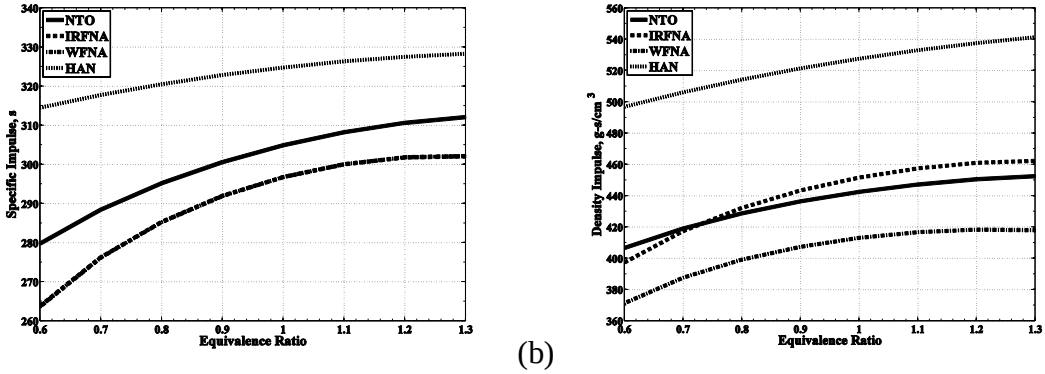

Figure A-10: Fuel 8 $C_4H_9N_9$ combined with select oxidizers versus equivalence ratio
(a) Performance measured in specific impulse
(b) Performance measured in density impulse

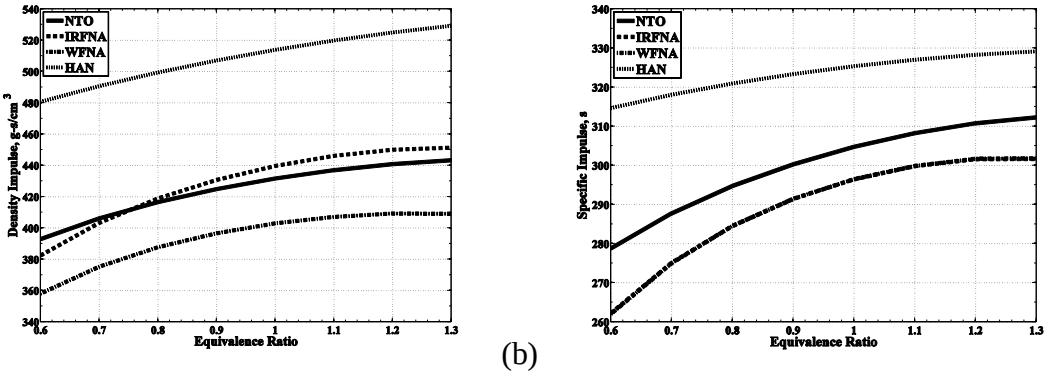

Figure A-11: Fuel 9 $C_5H_{11}N_9$ combined with select oxidizers versus equivalence ratio
(a) Performance measured in specific impulse
(b) Performance measured in density impulse

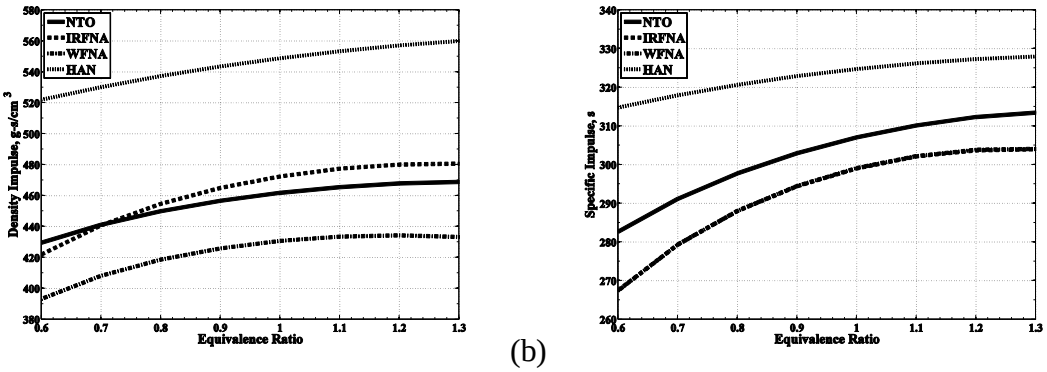

Figure A-12: Fuel 9 $C_3H_9N_{11}$ combined with select oxidizers versus equivalence ratio
(a) Performance measured in specific impulse
(b) Performance measured in density impulse

APPENDIX B.
IONIC LIQUID PROPERTY DATA

Table B-1. Electrochemical property data for ionic liquids

Ionic Liquid Name	1-butylpyridinium bistrifluoromethyl sulfonylimide	butyltrimethylammonium bistrifluoromethyl sulfonylimide	1,3-dimethylimidazolium bistrifluoromethyl sulfonylamide	hexyltrimethylammonium bistrifluoromethyl sulfonylimide
Formula	$C_{11}H_{14}F_6N_2O_4S_2$	$C_9H_{18}F_6N_2O_4S_2$	$C_7H_9F_6N_3O_4S_2$	$C_{11}H_{22}F_6N_2O_4S_2$
Formula Cation	$C_9H_{14}N$	$C_7H_{18}N$	$C_5H_9N_2$	$C_9H_{22}N$
Formula Anion	$C_2F_6NO_4S_2$	$C_2F_6NO_4S_2$	$C_2F_6NO_4S_2$	$C_2F_6NO_4S_2$
Molecular Weight Cation, g/mol	136.22	116.23	97.14	144.28
Molecular Weight Anion, g/mol	280.15	280.15	280.15	280.15
Conductivity, S/m	0.33±0.03 [41]	0.21±0.02 [41]	0.89± 0.01 [41, 47]	0.043± 0.004 [49]
Melting Temperature, K	299.1± 1 [41]	290.6±2.1 [41, 43]	299±1 [41, 47]	
Density, kg/m^3	1449±15 [41]	1387.23± 10.87 [41, 44, 45]	1564.6±9.2 [41, 47, 48]	1310.64± 9.6 [44]
Viscosity, Pa*s		0.10565±.01 [41, 46]	0.038± 0.002 [41]	
Surface Tension, N/m		0.035255±.004 [44, 45]		0.0361±0.001 [44]
Static Dielectric	11.5 [42]			

Table B-2. Electrochemical property data for ionic liquids

Ionic Liquid Name	heptyltrimethylammonium bistrifluoromethyl sulfonylimide	trimethyloctylammonium bistrifluoromethyl sulfonylimide	triethylhexylammonium bistrifluoromethyl sulfonylimide	1-ethyl-3-methylimidazolium bistrifluoromethyl sulfonylimide
Formula	$C_{12}H_{24}F_6N_2O_4S_2$	$C_{13}H_{26}F_6N_2O_4S_2$	$C_{14}H_{28}F_6N_2O_4S_2$	$C_8H_{11}F_6N_3O_4S_2$
Formula Cation	$C_{10}H_{24}N$	$C_{11}H_{26}N$	$C_{12}H_{28}N$	$C_6H_{11}N_2$
Formula Anion	$C_2F_6NO_4S_2$	$C_2F_6NO_4S_2$	$C_2F_6NO_4S_2$	$C_2F_6NO_4S_2$
Molecular Weight Cation, g/mol	158.31	172.33	186.36	111.17
Molecular Weight Anion, g/mol	280.15	280.15	280.15	280.15
Conductivity, S/m	0.04±0.004 [49]	0.035±0.007 [49]	0.067±0.005 [49]	0.91085±0.001 [41, 47, 50]
Melting Temperature, K			293.1±2.0 [49]	255.85±0.96 [41, 43, 47, 51]
Density, kg/m^3	1280±30 [49]	1270±30 [49]	1279.3±9.20 [44]	1520.8±2.8 [41,45,47,48,52]
Viscosity, Pa*s		0.181±0.02 [49]	0.167±0.019 [49]	0.0333 ±0.0011[41, 53,54]
Surface Tension, N/m			0.03544±0.0001 [44]	0.038018 [44, 45, 55]
Static Dielectric				12.3 [42]

Table B-3. Electrochemical property data for ionic liquids

Ionic Liquid Name	1-hexyl-3-methylimidazolium bistrifluoromethyl sulfonylimide	triethylheptylammonium bistrifluoromethyl sulfonylimide	triethyloctylammonium bistrifluoromethyl sulfonylimide	tributylhexylammonium bistrifluoromethyl sulfonylimide
Formula	$C_{12}H_{19}F_6N_3O_4S_2$	$C_{15}H_{30}F_6N_2O_4S_2$	$C_{16}H_{32}F_6N_2O_4S_2$	$C_{20}H_{40}F_6N_2O_4S_2$
Formula Cation	$C_{10}H_{19}N_2$	$C_{13}H_{30}N$	$C_{14}H_{32}N$	$C_{18}H_{40}N$
Formula Anion	$C_2F_6NO_4S_2$	$C_2F_6NO_4S_2$	$C_2F_6NO_4S_2$	$C_2F_6NO_4S_2$
Molecular Weight Cation, g/mol	167.28	200.39	214.42	270.52
Molecular Weight Anion, g/mol	280.15	280.15	280.15	280.15
Conductivity, S/m	0.219±0.003 [36,42,45,51,52]	0.051±0.003 [44]	0.033±0.002 [44]	0.016±0.002 [44]
Melting Temperature, K	268.352±2.92 [36, 42, 48, 53]		287.1±4.0 [44]	299.1±2.0 [44]
Density, kg/m^3	1370.66±1.56 [36, 42, 52, 54-59]	1260±30 [44]	1250±20 [44]	1150±20.0 [44]
Viscosity, Pa*s	0.0715±0.004 [36, 42, 48-49, 51-52, 54, 59]	0.0755±0.008 [44]	0.202±0.0023 [44]	0.595±0.078 [44]
Surface Tension, N/m	0.0329±0.0021 [39, 59-60]			
Static Dielectric				

Table B-4. Electrochemical property data for ionic liquids

Ionic Liquid Name	tributylheptylammonium bistrifluoromethyl sulfonylimide	tributyloctylammonium bistrifluoromethyl sulfonylimide	ethylheptyl-di-1-methylethylammonium bistrifluoromethyl sulfonylimide	1-butyl-3-methylimidazolium bistrifluoromethyl sulfonylimide
Formula	$C_{21}H_{42}F_6N_2O_4S_2$	$C_{22}H_{44}F_6N_2O_4S_2$	$C_{17}H_{34}F6N2O4S2$	$C_{10}H_{15}F_6N_3O_4S_2$
Formula Cation	$C_{19}H_{42}N$	$C_{20}H_{44}N$	$C_{15}H_{34}N$	$C_8H_{15}N_2$
Formula Anion	$C_2F_6NO_4S_2$	$C_2F_6NO_4S_2$	$C_2F_6NO_4S_2$	$C_2F_6NO_4S_2$
Molecular Weight Cation, g/mol	284.55	298.58	228.44	139.22
Molecular Weight Anion, g/mol	280.15	280.15	280.15	280.15
Conductivity, S/m	0.016±0.001 [49]	0.013±0.003 [49]	0.031±0.0002 [49]	0.394±0.013 [41, 50, 66]
Melting Temperature, K				270±2 [41, 43, 47, 51, 67-68]
Density, kg/m^3	1170±20.0 [49]	1120±30.0 [49]	1270±20.0 [49]	1440± 13 [41, 45-48, 51, 61, 67, 69-72]
Viscosity, Pa*s	0.606±0.08 [49]	0.574±0.075	0.362±0.044 [49]	0.06± 0.01[41, 46, 47, 69, 72, 73]
Surface Tension, N/m				0.0346±0.003 [45, 55, 69]
Static Dielectric				

Table B-5. Electrochemical property data for ionic liquids

Ionic Liquid Name	N,N-dimethyl-N-propyl-1-butanaminium 1,1,1-trifluoro-N-trifluoromethyl sulfonylmethanesulfonamide	1-pentyl-3-methylimidazolium bistrifluoromethyl sulfonylimide	trihexyltetradecylphosphonium bistrifluoromethyl sulfonylimide	1-hexyl-3,5-dimethylpyridinium bistrifluoromethyl sulfonylimide
Formula	$C_{11}H_{22}F_6N_2O_4S_2$	$C_{11}H_{17}F_6N_3O_4S_2$	$C_{34}H_{68}F_6NO_4PS_2$	$C_{15}H_{22}F_6N_2O_4S_2$
Formula Cation	$C_9H_{22}N$	$C_9H_{17}N_2$	$C_{32}H_{68}P$	$C_{13}H_{22}N$
Formula Anion	$C_2F_6NO_4S_2$	$C_2F_6NO_4S_2$	$C_2F_6NO_4S_2$	$C_2F_6NO_4S_2$
Molecular Weight Cation, g/mol	144.28	153.25	483.87	192.33
Molecular Weight Anion, g/mol	280.15	280.15	280.15	280.15
Conductivity, S/m				
Melting Temperature, K	293.1 ±4.0 [43]		306.1 ±1.0 [84]	283 ±3.0 [53]
Density, kg/m^3	1348.3 ±10 [44]	1404.45 ±2.3 [83]	1050.1 ±2.4 [44]	
Viscosity, Pa*s				0.104 ±0.0006 [53]
Surface Tension, N/m	0.03838 ±0.001 [44]	0.032655 ± 0.0006 [44]	0.03308 ±0.0007[44]	
Static Dielectric				

Table B-6. Electrochemical property data for ionic liquids

Ionic Liquid Name	1-hexyl-3-methyl-4-(dimethylamino)pyridinium bistrifluoromethyl sulfonylamide	1-butyl-nicotinic acid butyl ester bistrifluoromethyl sulfonylimide	1-hexyl-2,3-dimethylimidazolium bistrifluoromethyl sulfonylimide	1-decyl-3-methylimidazolium bistrifluoromethyl sulfonylimide
Formula	$C_{16}H_{25}F_6N_3O_4S_2$	$C_{16}H_{22}F_6N_2O_6S_2$	$C_{13}H_{21}F_6N_3O_4S_2$	$C_{16}H_{23}F_6N_3O_4S_2$
Formula Cation	$C_{14}H_{25}N_2$	$C_{14}H_{22}NO_2$	$C_{11}H_{21}N_2$	$C_{14}H_{27}N_2$
Formula Anion	$C_2F_6NO_4S_2$	$C_2F_6NO_4S_2$	$C_2F_6NO_4S_2$	$C_2F_6NO_4S_2$
Molecular Weight Cation, g/mol	221.37	236.34	181.30	223.38
Molecular Weight Anion, g/mol	280.15	280.15	280.15	280.15
Conductivity, S/m				
Melting Temperature, K	271±3.0 [53]	288±3.0 [53]	268±3.0 [53]	
Density, kg/m^3				1278±2.4 [85]
Viscosity, Pa*s	0.112±0.007 [53]	0.531±0.056 [53]	0.131±0.009 [53]	0.1097±0.002 [54]
Surface Tension, N/m				
Static Dielectric				

Table B-7. Electrochemical property data for ionic liquids

Ionic Liquid Name	1-methyl-3-octylimidazolium hexafluorophosphate	1-hexyl-3-methylimidazolium tetrafluoroborate	1-methyl-3-octylimidazolium tetrafluoroborate	1-butyl-3-methylimidazolium tetrafluoroborate
Formula	$C_{12}H_{23}F_6N_2P$	$C_{10}H_{19}BF_4N_2$	$C_{12}H_{23}BF_4N_2$	$C_8H_{15}BF_4N_2$
Formula Cation	$C_{12}H_{23}N_2$	$C_{10}H_{19}N_2$	$C_{12}H_{23}N_2$	$C_8H_{15}N_2$
Formula Anion	F_6P	BF_4	BF_4	BF_4
Molecular Weight Cation, g/mol	195.33	167.28	195.33	139.22
Molecular Weight Anion, g/mol	144.96	86.80	86.80	86.80
Conductivity, S/m	0.025686±0.0005 [115]	0.1228±0.001 [86]	0.0587±0.001 [115]	0.354±0.005 [41, 86, 126]
Melting Temperature, K				
Density, kg/m^3	1232.96±6.19 [69, 72, 94, 96-100, 113-1114, 116]	1145.8196±1.44 [86, 111, 119-120]	1103.211± 5.38[78, 89, 121-124]	1199.953±9.81 [41, 46, 51, 69, 86, 95, 106-107, 117-118, 127
Viscosity, Pa*s	0.702± 0.028 [69, 98]	0.172125±0.05[54, 64, 118]	0.34002±.0015 [116, 118, 122, 125]	0.12398±0.037 [41, 46, 69,117-118, 127]
Surface Tension, N/m	0.04195±0.005[69, 117]	0.038±0.0017[64, 110]	0.0307±0.001 [110]	
Static Dielectric			10.1 [126]	

Table B-8. Electrochemical property data for ionic liquids

Ionic Liquid Name	1,3-diethylimidazolium bistrifluoromethyl sulfonylimide	1-hexylpyridinium bistriflurometh sulfonylimide	1-butyl-3-methylimidazolium hexafluorophosphate	1-hexyl-3-methylimidazolium hexafluorophosphate
Formula	$C_9H_{13}F_6N_3O_4S_2$	$C_{13}H_{18}F_6N_2O_4S_2$	$C_8H_{15}F_6N_2P$	$C_{10}H_{19}F_6N_2P$
Formula Cation	$C_7H_{13}N_2$	$C_{11}H_{18}N$	$C_8H_{15}N_2$	$C_{10}H_{19}N_2$
Formula Anion	$C_2F_6NO_4S_2$	$C_2F_6NO_4S_2$	F_6P	F_6P
Molecular Weight Cation, g/mol	125.19	178.28	139.22	167.28
Molecular Weight Anion, g/mol	280.15	280.15	144.96	144.96
Conductivity, S/m			0.1476±0.002 [41, 50, 86]	0.11±0.02 [59]
Melting Temperature, K	262.6±0.04 [83]	273±3.0 [53]	280.652±3.30 [41, 51, 67, 69, 87, 88]	
Density, kg/m^3	1469.6±9.05 [85]		1366.685±3.99 [41, 67, 69,72, 86, 89-107]	1290.84±5.79 [64, 69, 72, 96, 98, 100, 111-114]
Viscosity, Pa*s			0.2707519±0.0707 [41, 54, 69, 72, 73, 90, 98, 101, 108-109]	0.5145075±0.05 [54, 64, 69, 98]
Surface Tension, N/m	0.038±0.002 [55]	0.08±0.005 [53]	0.048044±0.0036 [44, 69, 98, 109-110]	0.0415±0.003 [64, 69, 98, 110]
Static Dielectric			11.4 [42]	

Table B-9. Electrochemical property data for ionic liquids

Ionic Liquid Name	1-propyl-3-methylimidazolium tetrafluoroborate	1-ethyl-3-methylimidazolium tetrafluoroborate	1-isobutenyl-3-methylimidazolium tetrafluoroborate	1-butylpyridinium tetrafluoroborate
Formula	$C_7H_{13}BF_4N_2$	$C_6H_{11}BF_4N_2$	$C_8H_{13}BF_4N_2$	$C_9H_{14}BF_4N$
Formula Cation	$C_7H_{13}N_2$	$C_6H_{11}N_2$	$C_8H_{13}N_2$	$C_9H_{14}N$
Formula Anion	BF_4	BF_4	BF_4	BF_4
Molecular Weight Cation, g/mol	125.19	111.17	122.17	136.22
Molecular Weight Anion, g/mol	86.80	86.80	86.80	86.80
Conductivity, S/m	0.59± 0.06 [121]	1.5385±0.1 [86, 127-128]		
Melting Temperature, K	256.1±1.0 [121]	286.835±1.04 [127,129]		279.79±0.05[130]
Density, kg/m^3	1240±20 [121]	1281.06±2.09 [86, 127-128]		1213.9±0.71[89, 131]
Viscosity, Pa*s	0.103±0.011 [121]	0.036535±0.0007 [127, 128]	0.1185±0.0046[109]	0.16326±0.0079 [131]
Surface Tension, N/m			0.0518±0.0022 [109]	
Static Dielectric		15 [126]		

Table B-10. Electrochemical property data for ionic liquids

Ionic Liquid Name	1-butyl-4-methylpyridinium tetrafluoroborate	1-(2-hydroxyethyl)-3-methylimidazolium tetrafluoroborate	1-butyl-2,3-dimethylimidazolium tetrafluoroborate	1-hexyl-3-methylimidazolium chloride
Formula	$C_{10}H_{16}BF_4N$	$C_6H_{11}N_2OBF_4$	$C_9H_{17}N_2BF_4$	$C_{10}H_{19}ClN_2$
Formula Cation	$C_{10}H_{16}N$	$C_6H_{11}N_2O$	$C_9H_{17}N_2$	$C_{10}H_{19}N_2$
Formula Anion	BF_4	BF_4	BF_4	Cl
Molecular Weight Cation, g/mol	150.24	127.17	153.25	167.28
Molecular Weight Anion, g/mol	86.80	86.80	86.80	35.45
Conductivity, S/m				
Melting Temperature, K				
Density, kg/m^3	1183.6725±0.73 [52, 132-134]	1308±4.1 [125]	1191.2±8.0 [136]	1036.69±5.81 [69, 134, 138]
Viscosity, Pa*s	0.1962±0.073 [133]	0.974±0.17 [125]	0.45581±0.029 [51, 135-136]	0.716±0.069 [69]
Surface Tension, N/m				0.04215±0.00049 [69, 110]
Static Dielectric				

Table B-11. Electrochemical property data for ionic liquids

Ionic Liquid Name	trihexyl tetradecylphosphonium chloride	1-methyl-3-octylimidazolium chloride	1-butyl-3-methylimidazolium chloride	1-ethyl-3-methylimidazolium chloride
Formula	$C_{32}H_{68}ClP$	$C_{12}H_{23}ClN_2$	$C_8H_{15}ClN_2$	$C_6H_{11}ClN_2$
Formula Cation	$C_{32}H_{68}P$	$C_{12}H_{23}N_2$	$C_8H_{15}N_2$	$C_6H_{11}N_2$
Formula Anion	Cl	Cl	Cl	Cl
Molecular Weight Cation, g/mol	483.87	195.33	139.22	111.17
Molecular Weight Anion, g/mol	35.45	35.45	35.45	35.45
Conductivity, S/m				
Melting Temperature, K			340.535±0.94 [88,142-143]	358.1±4.0 [142]
Density, kg/m^3	882.6±2.80 [44]	1008.1±3.5 [69, 139-140]	1080±10 [69]	1186±4.0 [144]
Viscosity, Pa*s		0.337±0.003 [69, 137, 140		
Surface Tension, N/m	0.03362±0.0082 [69, 44]	0.033±0.001 [69, 141, 141	0.0482±0.0014 [110]	
Static Dielectric				

Table B-12. Electrochemical property data for ionic liquids

Ionic Liquid Name	1-butyl-3-methylimidazolium triflate	tributyloctylammonium trifluoromethanesulfonate	1-ethyl-3-methylimidazolium triflate	1-butyl-3-methylimidazolium dicyanamide
Formula	$C_9H_{15}F_3N_2O_3S$	$C_{21}H_{44}F_3NO_3S$	$C_7H_{11}F_3N_2O_3S$	$C_{10}H_{15}N_5$
Formula Cation	$C_8H_{15}N_2$	$C_{20}H_{44}N$	$C_6H_{11}N_2$	$C_8H_{15}N_2$
Formula Anion	CF_3O_3S	CF_3O_3S	CF_3O_3S	C_2N_3
Molecular Weight Cation, g/mol	139.22	298.58	111.17	139.22
Molecular Weight Anion, g/mol	149.07	149.07	149.07	66.04
Conductivity, S/m	0.29±0.03 [41]	0.0017±0.0002 [49]		1.139±0.011 [86]
Melting Temperature, K	286.1±1.0 [41, 51]		262.23±0.06 [145]	267.1±1.0 [51]
Density, kg/m^3	1298.9±2.7 [41, 51, 107, 119]	1020±20 [49]	1384.6±0.9 [76,146-147]	1059.12±6.10 [86]
Viscosity, Pa*s	0.0844±0.0073 [41]	2.03±0.36[49]	0.041±0.002 [148]	
Surface Tension, N/m			0.044419±0.00059 [44]	
Static Dielectric	13.2 [126]		15.1 [126]	11.9 [42]

REFERENCES

[1] Lide, D. R., "CRC Handbook of Chemistry and Physics," 88th ed., Taylor and Francis Group, LLC, 2008, pp. 6.153-6.156.

[2] Zube, D., Wucherer, E., Reed, B., "Evaluation of Han-Based Propellant Blends," 39th AIAA Joint Propulsion Conference, AIAA Paper 2003-4643, 2003.

[3] Boatz, J., Gordon, M., Voth, G., Hammes-Schiffer, S., "Design of Energetic Ionic Liquids," DoD HPCMP Users Group Conference, Pittsburg, 2008, pp.196-200.

[4] Smiglak, M., Reichert, M.W., Holbrey, J. D., Wilkes, J. S., Sun, L., Thrasher, J. S., Kirichenko, K., Singh, S., Katritzky, A. R., Rogers, R. D., "Combustible ionic liquids by design: is laboratory safety another ionic liquid myth?," Chem. Commun., Issue 24, 2006, pp. 2554-2556.
doi: 10.1039/b602086k

[5] Amariei, D., Courtheoux, L., Rossignol, S., Batonneau, Y., Kappenstein, C., Ford, M., Pillet, N., "Influence of the fuel on the thermal and catalytic decompositions of ionic liquid monopropellants," 41st AIAA Joint Propulsion Conference, AIAA Paper 2005-3980, 2005.

[6] Chang, Y., Kuo, K., "Assessment of Combustion Characteristics and Mechanism of a HAN-Based Liquid Monopropellant," 37th Joint Propulsion Conference, AIAA Paper 2001-3272, 2001.

[7] Meng, M., Khare, P., Risha, G., Yetter, R.,Yang, V., "Decomposition and Ignition of HAN-Based Monopropellants by Electrolysis," 47th AIAA Aerospace Sciences Meeting, AIAA Paper 2009-451, 2009.

[8] Schneider, S., Hawkins, T., Rosander, M., Vaghjiani, G., Chambreau, S., Drake, G., "Ionic Liquids as Hypergolic Fuels," Energy & Fuels, Vol. 22, No. 4, 17 Jun. 2008, pp. 2871–2872.

[9] Gao, H., Joo, Y., Twamley, B., Shreeve, J., "Hypergolic Ionic Liquids with 2-2,Dialkyltiazanium Cation," Chemistry International, Vol. 121, No. 15, 5 Mar. 2009, pp. 2830 – 2833.
doi: 10.1002/ange.200900094

[10] Dambach, E., Heister, S., Ismail, I., Schneider, S., Hawkins, T., "An Investigation into the hypergolicity of Dicyanamide-Based Ionic Liquid Fuels with Common Oxidizers," JANNAF 4th Propulsion Meeting, Orlando, 2008.

[11] Lozano, P., Sanchez, M., "Efficiency Estimation of EMI-BF4 Ionic Liquid Thrusters," 41st AIAA Joint Propulsion Conference, AIAA Paper 2005-4388, 2005.

[12] Lozano, P., Glass, P., Sanchez, M., "Performance Characteristics of a Linear Ionic Liquid Electrospray Thruster," 29th International Electric Propulsion Conference, IEPC Paper 2005-192, 2005.

[13] Garoz, D., Bueno, C., Larriba, C., Castro, C., Ferna´ndez de la Mora, J., "Taylor cones of ionic liquids from capillary tubes as sources of pure ions for electrical propulsion," 42th AIAA Joint Propulsion Conference, AIAA Paper 2003-4846, 2006.

[14] Dominick, S., "Design, Development, and Flight Performance of the Mars Global Surveyor Propulsion System," 35th AIAA Joint Propulsion Conference, AIAA Paper A99-2176, 1999.

[15] Gordon, S., "Computer Program for Calculation of Complex Chemical Equilibrium Compositions and Applications," NASA RP-1311-P2, 1996.

[16] Emel'yanenko, V., Verevkin, S. P., Heintz, A., "The Gaseous Enthalpy of Formation of the Ionic Liquid 1-Butyl-3-methylimidazolium Dicyanamide from Combustion Calorimetry, Vapor Pressure Measurements, and Ab Initio Calculations," American Chemistry Society, Vol. 129 , No. 13, 13 Mar. 2007, pp. 3930-3937.
doi: 10.1021/ja0679174

[17] Emel'yanenko, V., Verevkin, S. P., Heintz, A.,, Corfield, J., Deyko, A., Lovelock, K. R. J., Licence, P., Jones, R. G., "Pyrrolidinium-Based Ionic Liquids.1-Butyl-3-methylpyrrolidinium Dicyanamide: Thermochemical Measurement, Mass Spectrometry, and Ab Initio Calculations," Journal of Physical Chemistry B, Vol. 112, No. 37, 26 Aug. 2008, pp. 11734-11742.
doi: 10.1021/jp803238t

[18] Tao, G., Guo, Y., Joo, Y., Twamley, B., Shreeve, J., "Energetic nitrogen-rich salts and ionic liquids: 5-aminotetrazole (AT) as a weak acid," Journal of Material Chemistry, Vol. 18, No. 45, 16 Oct. 2008, pp. 5524-5530.

[19] Sutton, G. P., Biblarz, O., "Rocket Propulsion Elements," 7th ed., Wiley-Interscience Publication, New York, 2001, pp. 45-101, 160-361.

[20] "CPIA/M5 Liquid Propellant Engine Manual," Johns Hopkins University, Columbia, MD. Chemical Propulsion Information Agency (1998).

[21] Fernandez de la Mora, J., "The Fluid Dynamics of Taylor Cones," Annual Review of Fluid Mechanics, Vol. 39, No. 1, Jan. 2007, pp. 217-243.
doi: 10.1146/annurev.fluid.39.050905.110159

[22] Fernandez de la Mora, J., "Ionic Propulsion Based on Heated Taylor Cones of Ionic Liquids," 39th AIAA Joint Propulsion Conference, AIAA Paper 2003-4846, 2003.

[23] Fernandez de la Mora, J., Loscertales, I., "The Current Emitted by Highly Conducting Taylor Cones," Journal of Fluid Mechanics, 1994, pp. 155-184.
doi:10.1017/S0022112094003472

[24] Chiu, Y., Dressler,A., "Ionic Liquids for Space Propulsion," In Ionic Liquids IV: ACS Symposium Series, Brennecke, J., Vol. 975, American Chemical Society, Washington, DC, 2007, pp. 138-160.
doi: 10.1021/bk-2007-0975.ch010

[25] Romero-Sanz, I., R. Bocanegra, R., Fernández de la Mora, J., Gamero-Castaño, M., "Source of heavy molecular ions based on Taylor cones of ionic liquids operating in the pure ion evaporation regimen," Journal of Applied Physics, Vol. 94, No. 6, 15 September 2003.
doi: 10.1063/1.1598281

[26] Guerrero, I., Bocanegra, R., Higuera, F. J., Fernández de la Mora, J., "Ion evaporation from Taylor cones of propylene carbonate mixed with ionic liquids," Journal of Fluid Mechanics, Vol. 591, 2007, pp. 437-459.
doi:10.1017/S0022112007008348

[27] Ganan-Calvo, A. M., "The Size and Charge of Droplets in the Electrospraying of Polar Liquids in Cone-jet mode, and the Minimum Droplet Size," Journal of Aerosol Sci., Vol. 28, No. 2, 1 Mar. 1997, pp. 249-275.
doi:10.1016/S0021-8502(96)00433-8

[28] Chen, D., Pui, D., "Experimental Investigation of Scaling Laws for Electrospraying: Dielectric Constant Effect," Aerosol Science and Technology, Vol. 27, No. 3, Sep. 1997, pp. 367 – 380.
doi: 10.1080/02786829708965479

[29] Ganan-Calvo, A., "On the General Scaling Theory for Electrospraying," Journal of Fluid Mechanics, Vol. 507, pp. 203-212.
doi: 10.1017/S0022112004008870

[30] Yoshida, Y., Baba, O., Saito, G., "Ionic Liquids Based on Dicyanamide Anion: Influence of Structural Variations in Cationic Structures on Ionic Conductivity," J. Phys. Chem. B, Vol. 111, No. 18. 18 Jan. **doi:** 10.1021/jp067055t

[31] Larriba, C., Yoshida, Y., Fernández de la Mora, J., "Correlation between Surface Tension and Void Fraction in Ionic Liquids," J. Phys. Chem. B., Vol. 112. No. 39, 12 Aug. 2008, pp. 12401–12407.
doi: 10.1021/jp8027929

[32] Garzo, D., Bueno, C., Larriba, C., Castro, S., Romero-Sanz, I., Fernández de la Mora, J., Yoshida, Y., Saito, G., "Taylor cones of ionic liquids from capillary tubes as sources of pure ions: The role of surface tension and electrical conductivity," Journal of Applied Physics, Vol. 102, No. 6, 28 Sep. 2007.
doi:10.1063/1.2783769

[33] Hurby, V., Monheiser, J., Pote, B., Freeman, C., Connolly, W., "Low Power, Hall Thruster Propulsion System," 26th International Electric Propulsion Conference, IEPC Paper 1999-092, 1999.

[34] Larson, W. J., and Wertz, J. R., "Space Mission Analysis and Design," 3rd ed., Microcosm Press, Springer, New York, 1999, pp. 711.

[35] Muller, J., "Thruster Options for Microspacecraft: A Review and Evaluation of Existing Hardware and Emerging Technologies," AIAA Paper 97-3058, 1997.

[36] Manzella, D., et al., "Evaluation of Low Power Hall Thruster Propulsion," AIAA Paper 96-2736, July 1996.

[37] Pinero, L. R., Hopson, M., Todd, P. C., Wong, B., "Performance of NEXT Engineering Model Power Processing Unit," AIAA Paper 2007-5214, 2007.

[38] Patterson, M. J., Oleson, S. R., "Low Power Propulsion for Small Spacecraft," AIAA Paper 97-3060, 1997.

[39] Humble, R. W., Henry, N. G., Larson, W. J., "Space Propulsion Analysis and Design," Revised., Primis Custom Publishing, New York, 1995, pp. 179-294.

[40] Cengel, Y. A., and Boles, M. A., "Thermodynamics an Engineering Approach," 4th ed., McGraw Hill, Boston, 2002, pp. 94-95.

[41] Tokuda, H., Tsuzuki, S., Susan, M. A. B. H., Hayamizu, K., Watanabe, M, "How Ionic Are Room-Temperature Ionic Liquids? An Indicator of the Physicochemical Properties," J. Phys. Chem. B., Vol. 110, No. 39, 6 Sep. 2006, pp. 19593-19600.
doi: 10.1021/jp064159v

[42] Weingärtner, H., "The Static Dielectric Constant of Ionic Liquids," Z. Phys. Chem., Vol. 220, No. 11-12, Oct. 2006, pp. 1395–1405.
doi: 10.1524/zpch.2006.220.10.1395

[43] MacFarlane, D. R., Meakin, P., Amini, N., Forsyth, M., "Structural studies of ambient temperature plastic crystal ion conductors," J. Phys. Condens. Matter, Vol. 13, No. 36, 2001, pp. 8257-8267.
doi: 10.1088/0953-8984/13/36/303

[44] Kilaru, P., Baker, G. A., Scovazzo, P., “Density and Surface Tension Measurements of Imidazolium-, Quaternary Phosphonium-, and Ammonium-Based Room-Temperature Ionic Liquids: Data and Correlations,” J. Chem. Eng. Data., Vol. 52, No. 2, 2008, pp. 613-621.
doi: 10.1021/je800030s

[45] Wandschneider, A., Lehmann, J. K., Heintz, A., “Surface Tension and Density of Pure Ionic Liquids and Some Binary Mixtures with 1-Propanol and 1-Butanol,” J. Chem. Eng. Data., Vol. 53, No. 2, 15 Jan. 2008, pp. 596-599.
doi: 10.1021/je700621d

[46] Jacquemin, J., Husson, P., Padua, A. A. H., Majer, V., “Density and viscosity of several pure and water-saturated ionic liquids,” Green Chem., Vol. 8, 2006, pp. 172-180.
doi: 10.1039/b513231b

[47] Tokuda, H., Hayamizu, K., Ishii, K., Susan, M. A. B. H.,Watanabe, M., "Physicochemical Properties and Structures of Room Temperature Ionic Liquids. 2. Variation of Alkyl Chain Length in Imidazolium Cation," J. Phys. Chem. B., Vol. 109, No. 13, 12 Mar. 2005, pp. 6103-6110.
doi: 10.1021/jp047480r

[48] Krummen, M., Wasserscheid, P., Gmehling J., “Measurement of Activity Coefficients at Infinite Dilution in Ionic Liquids Using the Dilutor Technique,” J. Chem. Eng. Data., Vol. 47, No. 6, 23 Oct. 2002, pp. 1411-1417.
doi: 10.1021/je0200517

[49] Sun, J., Forsyth, M., MacFarlane, D. R., “Room-Temperature Molten Salts Based on the Quaternary Ammonium Ion,” J. Phys. Chem. B., Vol. 102, No. 44, 8 Oct. 1998, pp. 8858-8864.
doi: 10.1021/jp981159p

[50] Widegren, J. A., Saurer, E. M., Marsh, K. N., Magee, J. W., "Electrolytic conductivity of four imidazolium-based room-temperature ionic liquids and the effect of a water impurity," J. Chem. Thermodyn., Vol. 37, No. 6, Jun. 2005, pp. 569-575.
doi:10.1016/j.jct.2005.04.009

[51] Fredlake, C. P., Crosthwaite, J. M., Hert, D. G., Aki, S. N. V. K., Brennecke, J. F., “Thermophysical properties of imidazolium-based ionic liquids,” J. Chem. Eng. Data., Vol. 49, No. 4, 10 Jun. 2004, pp. 954-964.
doi: 10.1021/je034261a

[52] Heintz, A., Kulikov, D. V., Verevkin, S. P., “Thermodynamic Properties of Mixtures Containing Ionic Liquids. 2. Activity Coefficients at Infinite Dilution of Hydrocarbons and Polar Solutes in 1-Methyl-3-ethyl-imidazolium Bis(trifluoromethyl-sulfonyl) Amide and in 1,2-Dimethyl-3-ethyl-imidazolium Bis(trifluoromethyl-sulfonyl) Amide Using Gas-Liquid Chromatography,” J. Chem. Eng. Data., Vol. 47, No. 4, 7 May 2002, pp. 894-899.
doi: 10.1021/je0103115

[53] Crosthwaite, J. M., Muldoon, M. J., Dixon, J. K.,Anderson, J. L., Brennecke, J. F., “Phase transition and decomposition temperatures, heat capacities and viscosities of pyridinium ionic liquids,” J. Chem. Thermodyn., Vol. 37, No. 6, Jun. 2005, pp. 559-568.
doi:10.1016/j.jct.2005.03.013

[54] Ahosseini, A., Scurto, A. M., “Viscosity of Imidazolium-Based Ionic Liquids at Elevated Pressures: Cation and Anion Effects,” Int. J. Thermophys., Vol. 29, No. 4 Aug. 2004, pp. 1222-1243.
doi: 10.1007/s10765-008-0497-7

[55] Carvalho, P. J., Freire, M. G., Marrucho, I. M., Queimada, A. J., "Surface Tensions for the 1-Alkyl-3-methylimidazolium Bis(trifluoromethylsulfonyl)imide Ionic Liquids," J. Chem. Eng. Data., Vol. 53, No. 6, 16 May 2008, pp. 1346-1350.
doi: 10.1021/je800069z

[56] Widegren, J. A., Magee, J. W., "Density, Viscosity, Speed of Sound, and Electrolytic Conductivity for the Ionic Liquid 1-Hexyl-3-methylimidazolium Bis(trifluoromethylsulfonyl)imide and Its Mixtures with Water," J. Chem. Eng. Data., Vol. 52, No. 6, 29 Sep. 2007, pp. 2331-2338.
doi: 10.1021/je700329a

[57] Kandil, M. E., Marsh, K. N., Goodwin, A. R. H., "Measurement of the Viscosity, Density, and Electrical Conductivity of 1-Hexyl-3-methylimidazolium Bis(trifluorosulfonyl)imide at Temperatures between (288 and 433) K and Pressures below 50 Mpa," J. Chem. Eng. Data., Vol. 52, No. 6, 26 Oct. 2007, pp. 2382-2387.
doi: 10.1021/je7003484

[58] Shevelyova, M. P., Zaitsau, D. H., Paulechka, Y. U., Blokhin, A. V., Kabo, G. J., "Solid-Liquid Equilibrium and Activity Coefficients for Caprolactam + 1-Hexyl-3-methylimidazolium Bis(trifluoromethylsulfonyl)imide and Cyclohexanone Oxime + 1-Hexyl-3-methylimidazolium Bis(trifluoromethylsulfonyl)imide," J. Chem. Eng. Data., Vol. 52, No. 4, 12 May 2007, 1360-1365.
doi: 10.1021/je7000683

[59] Fitchett, B. D., Knepp, T. N., Conboy, J. C., "1-Alkyl-3-methylimidazolium Bis(perfluoroalkylsulfonyl)imide Water-Immiscible Ionic Liquids," J. Electrochem. Soc., Vol. 151, No. 8, 8 July 2005, pp. E219-E225.
doi: 10.1149/1.1945567

[60] Kato, R., Gmehling, J., "Systems with ionic liquids: Measurement of VLE and c1 data and prediction of their thermodynamic behavior using original UNIFAC, mod. UNIFAC(Do) and COSMO-RS(Ol)," J. Chem. Thermodyn., Vol. 37, No. 6, Jun. 2005, pp. 603-619.
doi:10.1016/j.jct.2005.04.010

[61] de Azevedo, R. G., Esperanca, J. M. S. S., Szydlowski, J.; Visak, Z. P., Pires, P. F., Guedes, H. J. R., Rebelo, L. P. N., "Thermophysical and thermodynamic properties of ionic liquids over an extended pressure range: [bmim][NTf2] and [hmim][NTf2]," J. Chem. Thermodyn., Vol.37, No. 9, Sep. 2005, pp. 888-899.
doi:10.1016/j.jct.2005.04.018

[62] Lachwa, J., Morgado, P., Esperanca, J. M. S. S., Guedes, H. J. R., Lopes, J. N. C., Rebelo, L. P. N., "Fluid-Phase Behavior of {1-Hexyl-3-methylimidazolium Bis(trifluoromethylsulfonyl) Imide, [C6mim][NTf2], + C2-C8 n-Alcohol} Mixtures: Liquid-Liquid Equilibrium and Excess Volumes," J. Chem. Eng. Data., Vol. 51, No. 6, 3 Oct. 2006, pp. 2215-2221.
doi: 10.1021/je060307z

[63] Kumelan, J., Kamps, A. P. -S., Tuma, D., Maurer, G., "Solubility of CO2 in the ionic liquid [hmim][Tf2N]," J. Chem. Thermodyn., Vol. 38, No. 11, Nov. 2006, pp. 1396-1401.
doi:10.1016/j.jct.2006.01.013

[64] Muhammad, A., Mutalib, M. I. A., Wilfred, C. D., Murugesan, T., Shafeeq, A., "Thermophysical properties of 1-hexyl-3-methyl imidazolium based ionic liquids with tetrafluoroborate, hexafluorophosphate and bis(trifluoromethylsulfonyl)imide anions," J. Chem. Thermodyn., Vol. 40, No. 9, Sep. 2008, pp. 1433-1438.
doi:10.1016/j.jct.2008.04.016

[65] Carvalho, P. J., Freire, M. G., Marrucho, I. M., Queimada, A. J., Coutinho, J. A. P., "Surface Tensions for the 1-Alkyl-3-methylimidazolium Bis(trifluoromethylsulfonyl)imide Ionic Liquids," J. Chem. Eng. Data., Vol. 53, No. 6, 16 May 2006, pp. 1346-1350.

[66] Martino, W., de la Mora, F.J., Yoshida, Y., Saito, G., Wilkesc, J., "Surface tension measurements of highly conducting ionic liquids," Green Chem., Vol. 8, 25 Jan. 2006, pp. 390–397.
doi: 10.1039/b515404a

[67] Troncoso, J., Cerdeirina, C. A., Sanmamed, Y. A., Romani, L., Rebelo, L. P. N., "Thermodynamic Properties of Imidazolium-Based Ionic Liquids: Densities, Heat Capacities, and Enthalpies of Fusion of [bmim][PF6] and [bmim][NTf2]," J. Chem. Eng. Data., Vol. 51, No. 5, 2006, pp. 1856-1859.

[68] Shimizu, Y., Ohte, Y., Yamamura, Y., Saito, K., "Effects of Thermal History on Thermal Anomaly in Solid of Ionic Liquid Compound [C4mim][Tf2N]," Chem. Lett., Vol. 36, No. 12, 2007, pp. 1484.
doi:10.1246/cl.2007.1484

[69] Huddleston, J. G., Visser, A. E., Reichert, W. M., Willauer, H. D., Broker, G. A., Rogers, R. D., "Characterization and comparison of hydrophilic and hydrophobic room temperature ionic liquids incorporating the imidazolium cation," Green Chem., Vol. 3, 2001, pp.156-164.
doi: 10.1039/b103275p

[70] Jacquemin, J., Husson, P., Mayer, V., Cibulka, I., "High-Pressure Volumetric Properties of Imidazolium-Based Ionic Liquids: Effect of the Anion," J. Chem. Eng. Data., Vol. 52, No. 6, 6 Sep. 2007, pp. 2204-2211.
doi: 10.1021/je700224j

[71] Jacquemin, J., Husson, P., Majer, V., Gomes, M. F. C., "Influence of the Cation on the Solubility of CO2 and H2 in Ionic Liquids Based on the Bis(trifluoromethylsulfonyl)imide Anion," J. Solution Chem., Vol. 36, No. 8, Aug. 2008, pp. 967-979.
doi: 10.1007/s10953-007-9159-9

[72] Harris, K. R., Kanakubo, M., Woolf, L. A., "Temperature and Pressure Dependence of the Viscosity of the Ionic Liquids 1-Hexyl-3-methylimidazolium Hexafluorophosphate and 1-Butyl-3-methylimidazolium Bis(trifluoromethylsulfonyl)imide," J. Chem. Eng. Data., Vol. 52, No. 3, 2007, pp. 1080-1085.
doi: 10.1021/je700032n

[73] McFarlane, J., Ridenour, W. B., Luo, H., Hunt, R. D., DePaoli, D. W., "Room Temperature Ionic Liquids for Separating Organics from Produced Water," Sci. Technol., 40, 1245-1265.
doi: 10.1081/SS-200052807

[74] MacFarlane, D. R., Meakin, P.,Sun, J.; Amini, N., Forsyth, M., "Pyrrolidinium Imides: A New Family of Molten Salts and Conductive Plastic Crystal Phases," J. Phys. Chem. B., Vol. 103, No. 20, 26 Mar. 1999, pp. 4164-4170.

[75] Henderson, W. A., Passerini, S.,"Phase Behavior of Ionic Liquid- LiX Mixtures: PyrroIidinium Cations and TFSI- Anions," Chem. Mater., Vol. 16, No. 15, 1 Jul. 2004, pp. 2881-2885.
doi: 10.1021/cm049942j

[76] Gardas, R. L., Costa, H. F., Freire, M. G., Carvalho, P. J., Marrucho, I. M., Fonseca, I. M. A., Ferreira, A. G. M., Coutinho, J. A. P., "Densities and Derived Thermodynamic Properties of Imidazolium-, Pyridinium-, Pyrrolidinium-, and Piperidinium-Based Ionic Liquids," J. Chem. Eng. Data., Vol. 53, No. 3, 14 Feb. 2008, pp. 805-811.
doi: 10.1021/je700670k

[77] Zaitsau, D. H., Kabo, G. J., Strechan, A. A., Paulechka, Y. U., Tschersich, A., Verevkin, S. P., Heintz, A., "Experimental Vapor Pressures of 1-Alkyl-3-methylimidazolium Bis(trifluoromethylsulfonyl)imides and a Correlation Scheme for Estimation of Vaporization Enthalpies of Ionic Liquids ," J. Phys. Chem. A., Vol. 110, No. 22, 8 Jun. 2008, pp. 7303-7306.
doi: 10.1021/jp060896f

[78] Alonso, L., Arce, A., Francisco, M., Soto, A., "Measurement and Correlation of Liquid-Liquid Equilibria of Two Imidazolium Ionic Liquids with Thiophene and Methylcyclohexane," J. Chem. Eng. Data., Vol. 52, No. 6, 29 Sep. 2007, pp. 2409-2412.
doi: 10.1021/je700362q

[79] Alonso, L.,Arce, A., Francisco, M., Soto, A., "(Liquid + liquid) equilibria of [C8mim][NTf2] ionic liquid with a sulfur-component and hydrocarbons," J. Chem. Thermodyn., Vol. 40, No. 2, Feb. 2008, pp. 265-270.
doi:10.1016/j.jct.2007.06.016

[80] Alonso, L., Arce, A., Francisco, M., Soto, A., "Liquid-Liquid Equilibria for [C8mim][NTf2] + Thiophene + 2,2,4-Trimethylpentane or + Toluene," J. Chem. Eng. Data., Vol. 53, 1750-1755.
doi: 10.1021/je800071q

[81] Alonso, L., Arce, A., Francisco, M., Soto, A., "Phase behaviour of 1-methyl-3-octylimidazolium bis[trifluoromethylsulfonyl]imide with thiophene and aliphatic hydrocarbons: The influence of n-alkane chain length," Fluid Phase Equilib., Vol. 263, No. 2, 15 Feb. 2008, pp. 176-181.
doi: 10.1016/j.fluid.2007.10.010

[82] Andreatta, A. E., Arce, A., Rodil, E., Soto, A., "Physical Properties of Binary and Ternary Mixtures of Ethyl Acetate, Ethanol, and 1-Octyl-3-methyl-imidazolium Bis(trifluoromethylsulfonyl)imide at 298.15 K," J. Chem. Eng. Data., Vol. 54, No. 3, 11 Feb. 2009, pp. 1022.
doi: 10.1021/je800899w

[83] Domanska, U., Rekawek, A., Marciniak, A., “Solubility of 1-Alkyl-3-ethylimidazolium-Based Ionic Liquids in Water and 1-Octanol,” J. Chem. Eng. Data., Vol. 53, No. 5, 16 Apr. 2008, pp. 1126-1132.
doi: 10.1021/je700693z

[84] Arce, A., Earle, M. J., Katdare, S. P., Rodriguez, H., Seddon, K. R., “Phase equilibria of mixtures of mutually immiscible ionic liquids,” Fluid Phase Equilib., Vol. 261, No. 1-2, 1 Dec. 2007, pp. 427-433.
doi:10.1016/j.fluid.2007.06.017

[85] Tome, L. I. N., Carvalho, P. J., Freire, M. G., Marrucho, I. M., Fonseca, I. M. A., Ferreira, A. G. M., Coutinho, J. A. P., Gardas, R. L., “Measurements and Correlation of High-Pressure Densities of Imidazolium-Based Ionic Liquids,” J. Chem. Eng. Data., Vol. 53, pp. 1914-1921.
doi: 10.1021/je800316b

[86] Stoppa, A., Hunger, J., Buchner, R., “Conductivities of Binary Mixtures of Ionic Liquids with Polar Solvents.” J. Chem. Eng. Data., Vol. 54, No. 2, 25 Oct. 2009, pp. 472-479.
doi: 10.1021/je800468h

[87] Domanska, U., Marciniak, A., "Solubility of 1-Alkyl-3-methylimidazolium Hexafluorophosphate in Hydrocarbons," J. Chem. Eng. Data., Vol. 48, No. 3, 27 Feb. 2003, pp. 451-456.
doi: 10.1021/je020145g

[88] Domanska, U., Mazurowska, L., "Solubility of 1, 3-dialkylimidazolium chloride or hexafluorophosphate or methylsulfonate in organic solvents: effect of the anions on solubility," Fluid Phase Equilib., Vol. 221, No. 1-2, 30 Jul. 2004, pp. 73-82.
doi: 10.1016/j.fluid.2004.03.006

[89] Gu, Z., Brennecke, J. F., “Volume Expansivities and Isothermal Compressibilities of Imidazolium and Pyridinium-Based Ionic Liquids,” J. Chem. Eng. Data., Vol. 47, No. 2, 27 Feb. 2002, pp. 339-345.
doi: 10.1021/je010242u

[90] Kabo, G. J., Blokhin, A. V., Paulechka, Y. U., Kabo, A. G., Shymanovich, M. P., Magee, J. W., “Thermodynamic Properties of 1-Butyl-3-methylimidazolium Hexafluorophosphate in the Condensed State,” J. Chem. Eng. Data., Vol. 49, No. 3, 2004, pp. 453-461.
doi: 10.1021/je034102r

[91] Wang, J., Zhu, A., Zhuo, K., "Excess Molar Volumes and Excess Logarithm Viscosities for Binary Mixtures of the Ionic Liquid 1-Butyl-3-methylimidazolium Hexaflurophosphate with Some Organic Compounds," J. Solution Chem., Vol. 34, No. 5, May 2005, pp. 585-596.
doi: 10.1007/s10953-005-5594-7

[92] Kumelan, J., Kamps, A. P. -S., Tuma, D., Maurer, G., "Solubility of CO in the ionic liquid [bmim][PF6]," Fluid Phase Equilib., Vol. 228-229, Feb. 2005, pp. 207-211.
doi: 10.1016/j.fluid.2004.07.015

[93] Zafarani-Moattar, M. T., Shekaari, H., "Volumetric and Speed of Sound of Ionic Liquid, 1-Butyl-3-methylimidazolium Hexafluorophosphate with Acetonitrile and Methanol at T) (298.15 to 318.15) K," J. Chem. Eng. Data., Vol. 50, No. 5, 27 Jul. 2005, pp. 1694-1699.
doi: 10.1021/je050165t

[94] Tomida, D., Kumagai, A., Qiao, K., Yokoyama, C., "Viscosity of [bmim][PF6] and [bmim][BF4] at High Pressure," Int. J. Thermophys., Vol. 27, No. 1, Jan. 2006, pp. 39-47.
doi: 10.1007/s10765-006-0020-y

[95] Zafarani-Moattar, M. T., Shekaari, H., "Volumetric and compressibility behaviour of ionic liquid, 1-n-butyl-3-methylimidazolium hexafluorophosphate and tetrabutylammonium hexafluorophosphate in organic solvents at T = 298.15 K," J. Chem. Thermodyn., Vol. 38, No. 5, May 2006, pp. 624-633.
doi:10.1016/j.jct.2005.07.018

[96] Huo, Y., Xia, S., Ma, P., "Densities of Ionic Liquids, 1-Butyl-3-methylimidazolium Hexafluorophosphate and 1-Butyl-3-methylimidazolium Tetrafluoroborate, with Benzene, Acetonitrile, and 1-Propanol at T = (293.15 to 343.15) K," J. Chem. Eng. Data., Vol. 52, No. 5, 28 Jul. 2007, pp. 2077-2082.
doi: 10.1021/je700266n

[97] Pereiro, A. B., Rodriguez, A., "Experimental Liquid-Liquid Equilibria of 1-Alkyl-3-methylimidazolium Hexafluorophosphate with 1-Alcohols," J. Chem. Eng. Data., Vol. 52, No. 4, 8 May 2007, pp. 1408-1412.
doi: 10.1021/je700099w

[98] Pereiro, A. B., Legido, J. L., Rodriguez, A., "Physical properties of ionic liquids based on 1-alkyl-3-methylimidazolium cation and hexafluorophosphate as anion and temperature dependence," J. Chem. Thermodyn., Vol. 39, No. 8, Aug. 2008, pp. 1168-1175.
doi:10.1016/j.jct.2006.12.005

[99] Pereiro, A. B., Rodriguez, A., "Study on the phase behaviour and thermodynamic properties of ionic liquids containing imidazolium cation with ethanol at several temperatures," J. Chem. Thermodyn., Vol. 39, No. 6, Jun. 2007, pp. 978-989.
doi:10.1016/j.jct.2006.10.017

[100] Pereiro, A. B.,; Rodriguez, A., "Ternary (liquid + liquid) equilibria of the azeotrope (ethyl acetate + 2-propanol) with different ionic liquids at T = 298.15 K," J. Chem. Thermodyn., Vol. 39, No. 12, Dec. 2007, pp. 1608-1613.
doi:10.1016/j.jct.2007.04.010

[101] Zafarani-Moattar, M. T., Majdan-Cegincara, R., "Viscosity, Density, Speed of Sound, and Refractive Index of Binary Mixtures of Organic Solvent + Ionic Liquid, 1-Butyl-3-methylimidazolium Hexafluorophosphate at 298.15 K," J. Chem. Eng. Data., Vol. 52, 2359-2364.
doi: 10.1021/je700338t

[102] Kumar, A., "Estimates of Internal Pressure and Molar Refraction of Imidazolium Based Ionic Liquids as a Function of Temperature," J. Solution Chem., Vol. 37, No. 2, Feb. 2008, pp.203-214.
doi: 10.1007/s10953-007-9231-5

[103] Kumar, A., Singh, T., Gardas, R. L., Coutinho, J. A. P., "Non-ideal behaviour of a room temperature ionic liquid in an alkoxyethanol or poly ethers at T = (298.15 to 318.15) K," J. Chem. Thermodyn., Vol. 40, No. 1, Jan. 2008, pp. 32-39.
doi:10.1016/j.jct.2007.06.002

[104] Huo, Y., Xia, S., Ma, P., "Solubility of Alcohols and Aromatic Compounds in Imidazolium-Based Ionic Liquids," J. Chem. Eng. Data., Vol. 53, No. 11, 21 Oct. 2008, pp. 2535-2539.
doi: 10.1021/je800331n

[105] Hernandez-Fernandez, F. J., Gomez, D., Rubio, M., Tomas-Alonso, F., Villora, G., "Ternary liquid liquid equilibria for mixtures of an ionic liquid + n-hexane + an organic compound involved in the kinetic resolution of rac-1-phenyl ethanol (rac-1-phenyl ethanol, vinyl propionate, rac-1-phenylethyl propionate or propionic acid) at 298.2K and atmospheric pressure," Fluid Phase Equilib., Vol. 263, No. 2, 24, Oct. 2007, pp. 190-198.
doi: 10.1016/j.fluid.2007.10.011

[106] Qi, F., Wang, H., "Application of Prigogine Flory Patterson theory to excess molar volume of mixtures of 1-butyl-3-methylimidazolium ionic liquids with N-methyl-2-pyrrolidinone," J. Chem. Thermodyn., Vol. 41, No. 2, Feb. 2009, pp. 265-272.
doi: 10.1016/j.jct.2008.09.003

[107] Soriano, A. N., Doma Jr., B. T., Li, M. -H., "Measurements of the density and refractive index for 1-n-butyl-3-methylimidazolium-based ionic liquids," J. Chem. Thermodyn., Vol. 41, No. 3, Mar. 2009, pp. 301-307.
doi:10.1016/j.jct.2008.08.010

[108] Baker, S. N., Baker, G. A., Kane, M. A., Bright, F. V., "The Cybotactic Region Surrounding Fluorescent Probes Dissolved in 1-Butyl-3-methylimidazolium Hexafluorophosphate: Effects of Temperature and Added Carbon Dioxide," J. Phys. Chem. B., Vol. 105, No. 4, 31 Aug. 2001. pp. 9663-9668.
doi: 10.1021/jp0103528

[109] Jiqin, Z., Jian, C., Chengyue, L., Weiyang, F., "Viscosities and Interfacial Properties of I-Methyl-3-butylimidazolium Hexafluorophosphate and 1-Isobutenyl-3-methylimidazolium Tetrafluoroborate Ionic Liquids," J. Chem. Eng. Data., Vol. 52, No. 3, 14, Mar. 2007, pp. 812-816.
doi: 10.1021/je0604277

[110] Ghatee, M. H., Zolghadr, A. R., "Surface tension measurements of imidazolium-based ionic liquids at liquid vapor equilibrium," Fluid Phase Equilib., Vol. 263, No. 2, 15 Feb. 2008, pp. 168-175.
doi:10.1016/j.fluid.2007.10.004

[111] Letcher, T. M., Reddy, P., "Ternary liquid-liquid equilibria for mixtures of 1-hexyl-3-methylimidozolium (tetrafluoroborate or hexafluorophosphate) + ethanol + an alkene at T = 298.2K," Fluid Phase Equilib., Vol. 219, No. 2, 28 May 2004, pp. 107-112.
doi:10.1016/j.fluid.2003.10.012

[112] Pereiro, A. B., Tojo, E., Rodriguez, A., Canosa, J., Tojo, J., "Properties of ionic liquid HMIMPF6 with carbonates, ketones and alkyl acetates," J. Chem. Thermodyn., Vol. 38, No. 6, Jun. 2006, pp. 651-661.
doi:10.1016/j.jct.2005.07.020

[113] Pereiro, A. B., Rodriguez, A., "Thermodynamic Properties of Ionic Liquids in Organic Solvents from (293.15 to 303.15) K," J. Chem. Eng. Data., Vol. 52, No. 2, 25 Jan. 2007, pp. 600-608.
doi: 10.1021/je060497d

[114] Pereiro, A. B., Rodriguez, A., "A study on the liquid liquid equilibria of 1-alkyl-3-methylimidazolium hexafluorophosphate with ethanol and alkanes," Fluid Phase Equilib., Vol. 270, No. 1-2, 25 Aug. 2008, pp. 23-29.
doi:10.1016/j.fluid.2008.06.003

[115] Kanakubo, M., Harris, K. R.,Tsuchihashi, N., Ibuki, K., Ueno, M., "Temperature and pressure dependence of the electrical conductivity of the ionic liquids 1-methyl-3-octylimidazolium hexafluorophosphate and 1-methyl-3-octylimidazolium tetrafluoroborate," Fluid Phase Equilib., Vol. 261, No. 6, 5 Oct. 2007, pp. 414-420.
doi:10.1016/j.fluid.2007.06.019

[116] Harris, K. R., Kanakubo, M., Woolf, L. A., "Temperature and Pressure Dependence of the Viscosity of the Ionic Liquids 1-Methyl-3-octylimidazolium Hexafluorophosphate and 1-Methyl-3-octylimidazolium Tetrafluoroborate," J. Chem. Eng. Data., Vol. 51, No. 5, 18 Aug. 2005, pp. 1161-1167.
doi: 10.1021/je050147b

[117] Liu, W., Zhao, T., Zhang, Y., Wang, H., Yu, M., "The Physical Properties of Aqueous Solutions of the Ionic Liquid [BMIM][BF4]," J. Solution Chem., Vol. 35, No. 10, Oct. 2006, pp. 1337-1346.
doi: 10.1007/s10953-006-9064-7

[118] Sanmamed, Y. A., Gonzalez-Salagado, D., Troncoso, J., Cerdeirina, C. A.,Romani, L. , "Viscosity-induced errors in the density determination of room temperature ionic liquids using vibrating tube densitometry," Fluid Phase Equilib., Vol. 252, No. 1-2, 1 Mar. 2007, pp. 96-102.
doi:10.1016/j.fluid.2006.12.016

[119] Garcia-Miaja, G., Troncoso, J., Romani, L., "Excess properties for binary systems ionic liquid + ethanol: Experimental results and theoretical description using the ERAS model," Fluid Phase Equilib., Vol. 274, No. 1-2, 25 Dec. 2008, pp. 59-67.
doi:10.1016/j.fluid.2008.09.004

[120] Wagner, M., Stanga, O., Schroer, W., "The liquid liquid coexistence of binary mixtures of the room temperature ionic liquid 1-methyl-3-hexylimidazolium tetrafluoroborate with alcohols," Phys. Chem. Chem. Phys. , Vol. 6, No. 18, 2004, pp. 4421-4431.
doi: 10.1039/b404933k

[121] Heintz, A., Klasen, D., Lehmann, J. K., Wertz, C., "Excess Molar Volumes and Liquid-Liquid Equilibria of the Ionic Liquid 1-Methyl-3-Octyl-Imidazolium Tetrafluoroborate Mixed with Butan-1-ol and Pentan-1-ol," J. Solution Chem., Vol. 34, No. 10, Oct. 2005, pp. 1135-1144.
doi: 10.1007/s10953-005-7692-y

[122] Arce, A., Rodriguez, H., Soto, A., "Effect of anion fluorination in 1-ethyl-3-methylimidazolium as solvent for the liquid extraction of ethanol from ethyl tert-butyl ether," Fluid Phase Equilib., Vol. 242, No. 2, 25 Apr. 2006, pp. 164-168.
doi:10.1016/j.fluid.2006.01.008

[123] Alonso, L., Arce, A., Francisco, M., Rodriguez, O., Soto, A., “Liquid-Liquid Equilibria for Systems Composed by 1-Methyl-3-octylimidazolium Tetrafluoroborate Ionic Liquid, Thiophene, and n-Hexane or Cyclohexane,” J. Chem. Eng. Data., Vol. 52, No. 5, 6 Jul. 2007, pp. 1729-1732.
doi: 10.1021/je700126z

[124] Singh, T., Kumar, A., “Physical and excess properties of a room temperature ionic liquid (1-methyl-3-octylimidazolium tetrafluoroborate) with n-alkoxyethanols (C1Em, m = 1 to 3) at T = (298.15 to 318.15) K,” J. Chem. Thermodyn., Vol. 40, No. 3, mar. 2008, pp. 417-423.
doi:10.1016/j.jct.2007.09.011

[125] Restolho, J., Serro, A. P., Mata, J. L., Saramago, B., "Viscosity and Surface Tension of 1-Ethanol-3-methylimidazolium Tetrafluoroborate and 1-Methyl-3-octylimidazolium Tetrafluoroborate over a Wide Temperature Range," J. Chem. Eng. Data., Vol. 54, No. 3, 27 Jan. 2009, pp. 950-955.
doi: 10.1021/je800727f

[126] Singh, T., Kumar, A., “Static Dielectric Constant of Room Temperature Ionic Liquids: Internal Pressure and Cohesive Energy Denisty Approach,” J. Phys. Chem. B., Vol. 113, No. 41, 24 Sep. 2008, pp. 12968-12972.
doi: 10.1021/jp8059618

[127] Nishida, T., Tashiro, Y., Yamamoto, M., "Physical and electrochemical properties of 1-alkyl-3-methylimidazolium tetrafluoroborate for Electrolyte," J. Fluorine Chem., Vol. 120, No. 2, 1 Apr. 2003, pp. 135-141.
doi:10.1016/S0022-1139(02)00322-6

[128] Vila, J., Gines, P., Rilo, E., Cabeza, O., Varela, L. M., “Great increase of the electrical conductivity of ionic liquids in aqueous solutions,” Fluid Phase Equilib., Vol. 247, No. 1-2, 15 Sep. 2006, pp. 32-39.
doi:10.1016/j.fluid.2006.05.028

[129] Van Valkenburg, M. E., Vaughn, R. L., Williams, M., Wilkes, J. S., “Thermochemistry of ionic liquid heat-transfer fluids,” Thermochim. Acta, Vol. 425, No. 1-2, 20 Jan. 2005, pp.181-188.
doi:10.1016/j.tca.2004.11.013

[130] Zhang, Z.-H., Sun, L.-X., Tan, Z.-C., Xu, F., Lv, X.-C.,Zeng, J.-L., Sawada, Y., "THERMODYNAMIC INVESTIGATION OF ROOM TEMPERATURE IONIC LIQUID Heat capacity and thermodynamic functions of BPBF4," J. Therm. Anal. Calorim., Vol. 89, No. 3, Sep. 2006, pp. 289-294.
doi: 10.1007/s10973-006-7640-0

[131] Mokhtarani, B., Sharifi, A., Mortaheb, H. R., Mirzaei, M., Mafi, M.; Sadeghian, F., "Density and viscosity of pyridinium-based ionic liquids and their binary mixtures with water at several temperatures," J. Chem. Thermodyn., Vol. 41, No. 3, Mar. 2009, pp. 323-329.
doi:10.1016/j.jct.2008.09.001

[132] Heintz, A., Kulikov, D. V., Verevkin, S. P., "Thermodynamic Properties of Mixtures Containing Ionic Liquids. Activity Coefficients at Infinite Dilution of Alkanes, Alkenes, and Alkylbenzenes in 4-Methyl-n-butylpyridinium Tetrafluoroborate Using Gas-Liquid Chromatography," J. Chem. Eng. Data., Vol. 46, No. 6, 22 Sep. 2001, pp. 1526-1529.
doi: 10.1021/je0101348

[133] Heintz, A., Klasen, D., Lehmann, J. K., "Excess Molar Volumes and Viscosities of Binary Mixtures of Methanol and the Ionic Liquid 4-Methyl-N-butylpyridinium Tetrafluoroborate at 25, 40, and 50 deg C," J. Solution Chem., Vol. 31, No. 5, May 2005, pp. 467-476.
doi: 10.1023/A:1020217612751

[134] Ortega. J., Vreekamp, R., Penco, E., Marrero, E., "Mixing thermodynamic properties of 1-butyl-4-methylpyridinium tetrafluoroborate [b4mpy][BF4] with water and with an alkan-1ol (methanol to pentanol)," J. Chem. Thermodyn., Vol. 40, No. 7, Jul. 2007, pp. 1087-1094.
doi:10.1016/j.jct.2008.02.019

[135] Malham, I. B., Letellier, P., Mayaffre, A., Turmine, M.," Part I: Thermodynamic analysis of volumetric properties of concentrated aqueous solutions of 1-butyl-3-methylimidazolium tetrafluoroborate, 1-butyl-2,3-dimethylimidazolium tetrafluoroborate, and ethylammonium nitrate based on pseudo-lattice theory." J. Chem. Thermodyn., Vol. 39, No. 8, Aug. 2007, pp. 1132-1143.
doi:10.1016/j.jct.2007.01.007

[136] Malham, I. B., Turmine, M., "Viscosities and refractive indices of binary mixtures of 1-butyl-3-methylimidazolium tetrafluoroborate and 1-butyl-2,3-dimethylimidazolium tetrafluoroborate with water at 298 K," J. Chem. Thermodyn., Vol. 40, No. 4, Apr. 2008, pp. 718-723.
doi:10.1016/j.jct.2007.10.002

[137] Gomez, E., Gonzalez, B., Dominguez, A., Tojo, E., Tojo, J., "Dynamic Viscosities of a Series of 1-Alkyl-3-methylimidazolium Chloride Ionic Liquids and Their Binary Mixtures with Water at Several Temperatures," J. Chem. Eng. Data., Vol. 51, No. 2, 3 Feb. 2006, pp. 696-701.
doi: 10.1021/je050460d

[138] Gomez, E., Calvar, N., Dominguez, I., Dominguez, A., "Physical properties of the ternary mixture ethanol + water + 1-hexyl-3-methylimidazolium chloride at 298.15K," Phys. Chem. Liq., Vol. 44, No. 4, Aug. 2006, pp. 409-417.
doi: 10.1080/00319100600744993

[139] Letcher, D. W., Ramjugernath, T. M., Raal, J. D., "Activity coefficients of hydrocarbon solutes at infinite dilution in the ionic liquid, 1-methyl-3-octyl-imidazolium chloride from gas-liquid chromatography," J. Chem. Thermodyn., Vol. 35, No. 8, Aug. 2003, pp. 1335-1341.
doi:10.1016/S0021-9614(03)00091-0

[140] Gonzalez, E. J., Alonso, L., Dominguez, A., "Physical Properties of Binary Mixtures of the Ionic Liquid 1-Methyl-3-octylimidazolium Chloride with Methanol, Ethanol, and 1-Propanol at T = (298.15, 313.15, and 328.15) K and at P) 0.1 MPa," J. Chem. Eng. Data., Vol. 51, No. 4, 21 Jun. 2006, pp. 1446-1452.
doi: 10.1021/je060123k

[141] Law, G., Watson, P. R., "Surface Tension Measurements of N-Alkylimidazolium Ionic Liquids," Langmuir., Vol. 17, No. 20, 23 Aug. 2001, pp. 6138-6141.
doi: 10.1021/la010629v

[142] Wilkes, J. S., Levisky, J. A., Wilson, R. A., Hussey, C. L., "Dialkylimidazolium Chloroaluminate Melts: A New Class of Room-Temperature Ionic Liquids for Electrochemistry, Spectroscopy, and Synthesis," Inorg. Chem., Vol. 21, No. 3, Mar. 1982, pp. 1263-1264.
doi: 10.1021/ic00133a078

[143] Zhang, Q.-G., Xue, F., Tong, J., Guan, W., Wang, B., "Studies on Volumetric Properties of Concentrated Aqueous Solutions of the Ionic Liquid BMIBF4," J. Solution Chem., Vol. 35, No. 3, mar. 2006, pp. 297-309.
doi: 10.1007/s10953-005-9004-y

[144] Bolkan, S. A., Yoke, J. T., "Room Temperature Fused Salts Based on Copper(1) Chloride-I-Methyl-3-ethylOmidarolSum Chloride Mixtures. 1. Physical Properties," J. Chem. Eng. Data., Vol. 31, Apr. 1986, pp. 194-197.
doi: 10.1021/je00044a019

[145] Wachter, P., Schweiger, H.-G., Wudy, F., Gores, H. J., "Efficient determination of crystallisation and melting points at low cooling and heating rates with novel computer controlled equipment," J. Chem. Thermodyn., Vol. 40, No. 10, Oct. 2008, pp.1542-1547.
doi:10.1016/j.jct.2008.05.012

[146] Wong, C.-L., Soriano, A. N., Li, M. –H., "Diffusion coefficients and molar conductivities in aqueous solutions of 1-ethyl-3-methylimidazolium-based ionic liquids," Fluid Phase Equilib., Vol. 271, No. 1-2, 25 Oct. 2008, pp. 43-52.
doi:10.1016/j.fluid.2008.07.006

[147] Garcia-Miaja, G.. Troncoso, J., Romani, L., "Excess molar properties for binary systems of alkylimidazolium-based ionic liquids + nitromethane. Experimental results and ERAS-model calculations," J. Chem. Thermodyn., Vol. 41, No. 3, Mar. 2009, pp. 334-341.
doi:10.1016/j.jct.2008.09.002

[148] Rodriguez, H., Brennecke, J. F., "Temperature and Composition Dependence of the Density and Viscosity of Binary Mixtures of Water + Ionic Liquid," J. Chem. Eng. Data., Vol. 51, No. 6, 10, Oct. 2006, pp. 2145-2155.
doi: 10.1021/je0602824

VITA

Brian Russell Donius was born to Kenny Edwin and Alice June Donius on January 21, 1987 in St. Ann, Missouri. He attended public school through the 6th grade, when he was withdrawn to pursue home schooling. After three years, rather than attend public high school, Brian enrolled at Saint Louis Community College at the age of 15 to pursue general transfer credit in the engineering curriculum. At age 18 Brian was accepted to the University of Missouri Rolla. After three years he was awarded his Bachelors of Science in Aerospace Engineering.

In the fall 2008, Brian began attending graduate school at Missouri University of Science and Technology. Over the course of his enrollment he was awarded two summer internships. One at NASA Marshall Space Flight Center developing trade study tools for large propulsion systems. The second internship was at the Air Force Research Lab Edwards Air Force Base assisting in experiment development for electrospray propulsion. Brian graduated with his Master of Science in Aerospace Engineering in spring 2010.